SRNL-STI-2012-00040
Revision 0

Keywords: *Plutonium, Neptunium, Uranium, Technetium, Americium, hematite, magnetite, goethite, ferrihydrite, high-level tank waste,*

Retention: *Permanent*

Literature Review on the Sorption of Plutonium, Uranium, Neptunium, Americium and Technetium to Corrosion Products on Waste Tank Liners

Dien Li and Daniel I. Kaplan

February 2012

Savannah River National Laboratory
Savannah River Nuclear Solutions, LLC
Aiken, SC 29808

Prepared for the U.S. Department of Energy
under contract number DE-AC09-08SR22470.

DISCLAIMER

Printed in the United States of America

Prepared for
U.S. Department of Energy

REVIEWS AND APPROVALS

Dien Li, Co-author, Environmental Sciences Date

Daniel I. Kaplan, Co-author, Environmental Sciences Date

Scott H. Reboul, Technical Reviewer, Process Technology Programs Date

Heather H. Burns, Project Manager, E&CPT Research Programs Date

John J. Mayer, Manager, Environmental Sciences Date

Alice M. Murray, Manager, Environmental Science and Biotechnology Date

Sharon L. Marra, Manager, E&CPT Research Programs Date

Kent H. Rosenberger, SRR, Manager, Closure & Disposal Assessment Date

EXECUTIVE SUMMARY

The objective of this report was to conduct a literature review to determine whether Pu, U, Np, Am, and Tc would sorb to corrosion products on tank liners after the tank was filled with reducing grout (cementitious material containing slag to promote reducing conditions). There were no studies in the literature specifically designed to simulate SRS conditions of interest; *i.e.*, sorption of these radionuclides to corrosion products in the presence of reducing grout. One of the key ancillary parameters controlling sorption of these radionuclides is pH; this is especially true of Pu and U. A grouted tank pore water may have a pH >12 and is expected to maintain that pH for thousands of years. All literature sorption experiments were performed in pH <10.5 systems. Consequently some extrapolation is involved to predict what would happen in a cementitious – corrosion product environment of pH >12. Furthermore, few studies were found to investigate the radionuclides sorption under reducing conditions. In this document, information is tabulated about trends on how radionuclides sorbed onto corrosion products with respect to ancillary parameters, such as pH, initial radionuclide concentration, and solid phases. Also tabulated are distribution coefficients (K_ds) calculated from the observed sorption fractions and the applicable corrosion product concentrations. Based on the collected information, conclusions were then drawn to determine if conservative assumptions were made in the existing performance assessment (PA) that does not permit Pu, U, Np, Am and Tc to sorb to corrosion products on tank liners.

It is likely that tank liner corrosion products would significantly sorb Pu. Based on the literature review, Pu tended to have increased sorption with increasing pH between pH 3 and 10. At pH 10, Pu consists of carbonate and/or hydroxide complexes. It appears that the iron oxyhydroxide solid phases out compete these Pu complexes in an aqueous phase to promote Pu sorption at a moderate carbonate concentration; however, the carbonate alkalinity of >100 meq/L would decrease the Pu sorption onto goethite (α-FeOOH) (Sanchez *et al*. 1985).

It is unlikely that tank liner corrosion products would retain much uranyl, UO_2^{2+}, U in the oxidized state. Unlike Pu-hydroxy/carbonate complexes, it appears that uranyl forms complexes at higher pH values that are resistant to sorption by Fe-oxyhydroxides. Several studies conducted at pH 8 to 10 demonstrated that uranyl sorption decreased compared to lower pH systems. However, tank grout will create reducing conditions that will promote the reduction of UO_2^{2+} to U(IV) and by virtue of its tetra-valence, much greater total U sorption to corrosion products would be expected under reducing conditions. Information is lacking on how U(IV) would sorb to corrosion products at high pH; this is a specific area where experimental data may be especially useful.

Due to its higher stable oxidation state, it is not surprising that Np as neptunyl(V) (NpO_2^+) sorbs appreciably less than Pu(IV) to iron oxyhydroxides. As the pH increased between 5 and 10 the K_d values of neptunyl increased significantly. Additionally, there was no experimental data to indicate that the K_d values declined at higher pH values as was observed with uranyl due to carbonate complexes; however, some modeling work indicated the decreased adsorption of Np at higher pH (Wang and Anderko, 2001). Tank

grout may promote reducing conditions, which may promote reduction of Np(V) to Np(IV) and therefore greater sorption to corrosion products. Information is lacking on how Np(IV) would sorb to corrosion products at high pH values. Americium sorbs strongly at high pH values. There was an exceptionally strong pH dependence, as sorption K_d values increased from double digits to four or five digits as the pH increased from 3 to >8. Americium is not a redox sensitive element and therefore the K_d values would be approximately the same under reducing and older grout that has become oxidized. Pertechnetate, TcO_4^-, would not be retained by corrosion products due to surface charge repulsion of the Fe-oxyhydroxide at high pH and high competing anion concentrations. However, under reducing conditions, the TcO_4^- would readily convert to Tc(IV) and again, the tetravalent cation, Tc(IV) would be expected to sorb strongly under reducing conditions to the Fe-oxyhydroxides at high pH values. We are not aware of any Tc(IV) sorption experiments conducted at elevated pH values with Fe oxyhydroxides.

The present PA does not address any sorption to corrosion products in its conceptual geochemical model. Based on this literature review, it is a conservative assumption in the present PA not to include Pu, Am, and Np sorption to corrosion products. It is a conservative assumption in the present PA not to include Tc and U sorption during the period that the tanks are reduced (the first two aging stages), however laboratory information is necessary to confirm this expectation. It is reasonable for the PA to omit Tc and U sorption (K_d = ~0 mL/g) during oxidizing conditions (older grout).

TABLE OF CONTENTS

LIST OF TABLES

LIST OF FIGURES

LIST OF ABBREVIATIONS

CD	Charge Distribution
DOE	Department of Energy
EXAFS	Extended X-ray Absorption Fine Structure
PA	Performance Assessment
SRNL	Savannah River National Laboratory
SRS	Savannah River Site
XANES	X-ray Absorption Near-Edge Structure
XAS	X-ray absorption spectroscopy
XPS	X-ray photo electron spectroscopy

1.0 Introduction

The Savannah River Site (SRS) has conducted performance assessment (PA) calculations to determine the risk associated with closing liquid waste tanks. The PA estimates the risk associated with a number of scenarios, making various assumptions. Throughout all of these scenarios, it is assumed that the carbon-steel tank liners holding the liquid waste do not sorb the radionuclides. Tank liners have been shown to form corrosion products, such as Fe-oxyhydroxides (Wiersma and Subramanian 2002). Many corrosion products, including Fe-oxyhydroxides, at the high pH values of tank effluent, take on a very strong negative charge. Given that many radionuclides may have net positive charges, either as free ions or complexed species, it is expected that many radionuclides will sorb to corrosion products associated with tank liners.

1.1 Objective and Scope

The objective of this report was to conduct a literature review to investigate whether Pu, U, Np, Am and Tc would sorb to corrosion products on tank liners after they were filled with reducing grout (cementitious material containing slag to promote reducing conditions). The approach was to evaluate radionuclides sorption literature with iron oxyhydroxide phases, such as hematite (α-Fe_2O_3), magnetite (Fe_3O_4), goethite (α-FeOOH) and ferrihydrite ($Fe_2O_3 \cdot 0.5H_2O$). The primary interest was the sorption behavior under tank closure conditions where the tanks will be filled with reducing cementitious materials. Because there were no laboratory studies conducted using site specific experimental conditions, (*e.g.*, high pH and HLW tank aqueous and solid phase chemical conditions), it was necessary to extend the literature review to lower pH studies and non-cementitious conditions. Consequently, this report relied on existing lower pH trends, existing geochemical modeling, and experimental spectroscopic evidence conducted at lower pH levels. The scope did not include evaluating the appropriateness of K_d values for the Fe-oxyhydroxides, but instead to evaluate whether it is a conservative assumption to exclude this sorption process of radionuclides onto tank liner corrosion products in the PA model. This may identify another source for PA conservatism since the modeling did not consider any sorption by the tank liner.

2.0 Approach to Literature Review

A literature review was conducted with the objectives and scope identified in Section 1.1. The published literature on the sorption of Pu, U, Np, Am and Tc onto hematite (α-Fe_2O_3), magnetite (Fe_3O_4), goethite (α-FeOOH) and ferrihydrite ($Fe_2O_3 \cdot 0.5H_2O$) was searched, critically reviewed, and studied. Among the key experimental parameters and sorption parameters included in the tables are: radionuclide, spike concentration, pH, K_d values, % sorption, solid phase and its loading, aqueous phase and its ion strength, and comments. The K_d values and sorption percentages are important because they provide an important metric for comparison between conditions. But perhaps equally important, particularly since extrapolation to higher pH and tank conditions is necessary, are the comments containing the researcher's (experimentalists) understanding of the sorption

processes. Although the comments are not quantitative, they provide important insight into sorption mechanisms, the underpinnings for why sorption occurs.

K_d values and sorption percentages were not always presented in each paper, therefore they had to be calculated using the information provided in the literature. The sorption percent from Powell *et al*. (2004, 2005) are the actual data, but the sorption percent from all other references were estimated based on the published graphs, and the estimated errors for adsorption percentage were within 5%. The sorption coefficient, K_d (mL/g), are converted based on the sorption percent, sorbent mass, and solution volume:

$$K_d = \frac{(Ci - Cf)}{Cf} \times \frac{V}{M} \quad (1)$$

or

$$K_d = \frac{\%\ adsorbed}{\%\ in\ solution} \times \frac{V}{M} \quad (2)$$

where C_i and C_f are initial and final radionuclide concentrations in the solution before and after sorption at the specified equilibrium time, respectively, *V* is solution volume (mL), and *M* is sorbent mass (g) (Carbol and Engkvist 1997). In addition, the K_d data of Pu(IV) on hematite and goethite from Lu *et al.* (1998) are cited directly from this reference and the sorption percentages were converted using equations 1.

Although a 5% estimated error in adsorption percentage is reasonable, it can obviously have a major impact on the uncertainty of the K_d values, especially as the sorption percentages approach 0 or 100. For example, as the sorption fraction rises from 95% to 99%, which is compounded by the V/M ratio, the associated K_d rises by five times. Similarly, as the sorption rises from 99.0% to 99.9%, the K_d rises by an order of magnitude. For this reason, along with this discussion, the sorption percentages are reported to whole numbers below 100 (*i.e*., 0-99%), the near-complete sorption is reported as ~99%, and the K_d for near-complete sorption is reported with an "approximation" sign, based on the ~99% sorption value. The K_d values are reported up to three digits. However, because of the inherent uncertainties, it must be recognized that not all of the three digits are significant. It is also noted that some of the references identified the quantities of Fe-oxyhydroxides in units of m^2/L (*e.g*., Powell *et al.* 2004, 2005, Sanchez *et al*. 1985) or in M *(e.g*., Girvin *et al*. 1991, Hiemstra *et al*. 2009, Payne *et al*. 1998, Waite *et al*. 1994), which were converted to units of g/L for use in calculating the K_ds. In some cases, the assumptions made to support the unit conversions may have contributed additional uncertainty to the K_d values.

3.0 Results and Discussions

3.1 Plutonium

A summary of the plutonium sorption information (adsorption coefficient K_d, adsorption percentage, initial Pu concentration, pH, ion strength, equilibrium time, and sorbent loading) to iron oxyhydroxide phases is given in Table 1.

Romanchuk *et al*. (2011) studied Pu sorption onto hematite colloids (11 m^2/L) at 10^{-14} M and 10^{-9} M Pu concentrations over the pH range 1-7. In this study, a wide range of Pu concentrations and two Pu isotopes were used. ^{237}Pu and ^{239}Pu was Pu(IV) in 2M HNO_3 stock solution; to prepare Pu(VI), small amount of $NaBrO_3$ was added for oxidation. Figure 1 shows that for both Pu(VI) and Pu(IV), <10% Pu sorption was observed at pH < 3, the Pu sorption increases with pH and the Pu species are completely up-taken by hematite at pH >5.5. Pu sorption, regardless of oxidation state, reaches equilibrium faster in solutions containing 10^{-14} M Pu than that containing 10^{-9} M Pu (10 days versus 25 days, respectively). At both Pu concentrations, the similarity of the sorption edges for Pu(IV) and Pu(VI) at steady-state indicates the reduction of Pu(VI). Solvent extraction results confirmed that Pu(IV) is associated with hematite colloids above pH 5. The authors did not know what caused Pu redox transformations upon contact with hematite, but offered the following potential explanations: Pu redox transformations were due to (1) tracer amount of Fe(II) on hematite surface, (2) disproportionation of Pu(V), (3) electron shuttling from semiconducting hematite surface, or (4) self-reduction. The rate limiting step in Pu(VI) sorption is its surface-mediated reduction; the polymerization of Pu(IV) occurred on hematite surface.

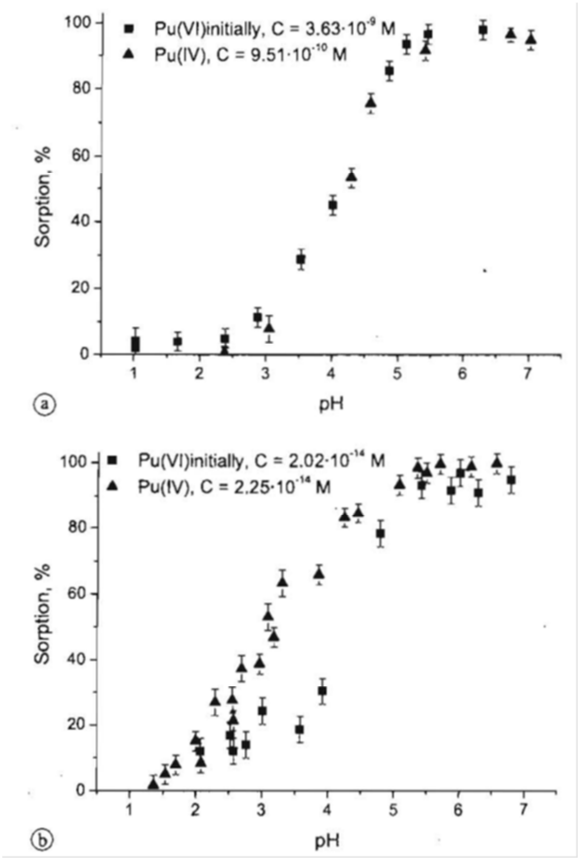

Figure 1. The pH sorption edges of Pu(VI) and Pu(IV) onto hematite at two different Pu total concentrations (Romanchuk *et al*. 2011).

Table 1. Plutonium sorption to iron oxyhydroxide phases

Radio-nuclide	Sorbents	Solution	Ion strength	pH	K_d (mL/g)	Sorp-tion (%)	Equil time (hrs)	Reference / Description
Pu	Hematite BET 35 m^2/g 0.32 g/L or 11 m^2/L	Pu(VI) 3.63×10^{-9} M	0.1 M $NaClO_4$	2.8	386	11	600	Romanchuk *et al*. (2011). The ^{237}Pu and ^{239}Pu was Pu(IV) in 2M HNO_3 stock solution; to prepare Pu(VI), a small amount of $NaBrO_3$ was added for oxidation. The authors attribute Pu redox transformation occurred upon sorption due to (1) tracer amount of Fe(II) on hematite surface, (2) disproportionation of Pu(V), (3) electron shuttling from semi-conducting hematite surface, or (4) self-reduction. The rate limiting step in Pu(VI) sorption is its surface-mediated reduction; the polymerization of Pu(IV) occurred on hematite surface. The K_d increases from pH 2.8 to 7.0; above pH 6, the K_d was >30,000 mL/g.
				5.5	5.93×10^{4}	95		
				6.3	1.01×10^{5}	97		
		Pu(IV) 9.51×10^{-10} M	0.1 M $NaClO_4$	3.1	271	8		
				5.5	3.59×10^{4}	92		
				7.0	5.94×10^{4}	95		
	Hematite BET 35 m^2/g 0.32 g/L or 11 m^2/L	Pu(VI) 2.02×10^{-14} M	0.1 M $NaClO_4$	3.0	987	24	240	
				4.8	1.11×10^{4}	78		
				6.7	4.15×10^{4}	93		
		Pu(IV) 2.25×10^{-14} M	0.1 M $NaClO_4$	3.0	2.0×10^{3}	39		
				5.1	4.15×10^{4}	93		
				6.6	3.09×10^{5}	99		
Pu	Hematite BET 36.3 m^2/g 0.276 g/L or 10 m^2/L	Pu(V) 1.5×10^{-8} M	0.01 M NaCl	3	36	1	97	Powell *et al*. (2005) This is primarily a study of kinetics of oxidation state transformations and Pu sorption from the aqueous phase in the presence of iron oxides. At pH 3, little sorption and reduction of Pu(V) was observed
				5	6.17×10^{3}	63	118	
				6.5	1.77×10^{4}	83	73	
				8	1.17×10^{5}	97	97	
	1.38 g/L 50 m^2/L			8	7.19×10^{4}	99	2	
	2.76 g/L or 100 m^2/L			3	7	2	355	
				8	~3.58×10^{4}	~99	3	

Radio-nuclide	Sorbents	Solution	Ion strength	pH	K_d (mL/g)	Sorp-tion (%)	Equil time (hrs)	Reference / Description
								on either hematite or goethite. At pH 5-8, the overall removal of Pu(V) was found to be approximately second order with respect to hematite concentration. In contrast to hematite, Pu(V) sorption to goethite occurred rapidly relative to reduction. As pH increases from 3 to 8, the K_d values increased; at pH 9 the >100,000 mL/g.
Pu	Goethite BET 167.2 m^2/g 0.12 g/L or 20 m^2/L	Pu(V) 1.5×10^{-8} M	0.01 M NaCl	6.5	2.0×10^5	96	23	
				8	$\sim8.25\times10^5$	~99	24	
	Goethite 0.30 g/L or 50 m^2/L			3	68	2	315	
				8	3.3×10^5	99	25	
	Goethite 0.60 g/L or 100 m^2/L			5	8.14×10^3	83	25	
				6.5	5.39×10^4	97	24	
				8	$\sim1.65\times10^5$	~99	3	
	Goethite 2.99 g/L or 500 m^2/L			6.5	$\sim3.31\times10^4$	~99	24	
Pu	Magnetite BET 25.4 m^2/g 0.39 g/L or 10 m^2/L	Pu(V) 1.5×10^{-8} M	0.01 M NaCl	3	525	17	438	Powell *et al*. (2004) In the pH range of 5-8, sorption is rate-limiting step, and reduction is mediated by solid phase; at pH 3, reduction occurs in the aqueous phase. As pH values increased from pH 3 to 8, the K_d values increased; at pH 8 the K_d values were (+∞) (>300,000 mL/g).
				5	2.95×10^4	92	22	
				8	$\sim2.54\times10^5$	~99	24	
	Magnetite 3.94 g/L or 100 m^2/L			3	56	18	26	
				3	2.57×10^3	91	215	
				8	$\sim2.54\times10^4$	~99	2	
Pu	Goethite BET 51.8 m^2/g 0.55 g/L or 28.5 m^2/L	Pu(IV) 1×10^{-11} M	0.1 M $NaNO_3$	2.6	979	35	24	Sanchez *et al.* (1985) Ion strength increase does not influence Pu(IV) or Pu(V) sorption. In the presence of DOC, Pu(V) reduction occurred in solution; Pu(IV) sorption on goethite decrease. Increasing total alkalinity above 100 meq/L promoted
				4	7.27×10^3	80		
				6.2	3.46×10^4	95		
				9.0	$\sim1.8\times10^5$	~99		
	Goethite BET 51.8 m^2/g 0.55 g/L or 28.5 m^2/L	Pu(IV) 1×10^{-10} M	0.1 M $NaNO_3$	2.3	202	10	24	
				3.7	1.82×10^3	50		
				6.2	2.85×10^4	94		
	Goethite	Pu(V)	0.1 M	4	18	1	1	

Radio-nuclide	Sorbents	Solution	Ion strength	pH	K_d (mL/g)	Sorp-tion (%)	Equil time (hrs)	Reference / Description
	BET 51.8 m^2/g 0.55 g/L or 28.5 m^2/L	1×10^{-11} M	$NaNO_3$	6	346	16		Pu(IV) and Pu(V) desorption from goethite, with the alkalinity of 1000 meq/L totally inhibiting sorption due to the formation of Pu-CO_3 complex and competition of surface exchange site. Carbonate alkalinity: CT (meq/L) = $[HCO_3^-]$ + $2\times[CO_3^{2-}]$
				8	4.36×10^4	96		
				9	8.91×10^4	98		
				4	272	13	480	
				5.8	2.09×10^4	92		
				8	$\sim1.8\times10^5$	~99		
	Goethite BET 51.8 m^2/g 0.55 g/L or 28.5 m^2/L	Pu(V) 1×10^{-10} M	0.1 M $NaNO_3$	4	18	1	1	
				6	779	30		
				8	3.46×10^4	95		
				9.8	$\sim1.8\times10^5$	~99		
				4.6	372	17	480	
				5.9	5.76×10^3	76		
				7.0	2.09×10^4	92		
Pu	Goethite BET 51.8 m^2/g 0.55 g/L or 28.5 m^2/L	Pu(IV) 1×10^{-11} M CT: 10 meq/L		8.6	$\sim1.8\times10^5$	~99	96	
		CT: 110 meq/L		8.6	2.85×10^4	94		
		CT: 300 meq/L		8.6	1.49×10^3	45		
		CT: 1000 meq/L		8.6	56	3		
	Goethite BET 51.8 m^2/g 0.55 g/L or 28.5 m^2/L	Pu(V) 1×10^{-11} M CT: 10 meq/L		8.6	$\sim1.8\times10^5$	~99	168	
		CT: 110 meq/L		8.6	2.85×10^4	94		
		CT: 310 meq/L		8.6	1.75×10^3	49		
		CT: 1000 meq/L		8.6	37	2		
Pu	Hematite BET 53.5 m^2/g 0.5 g/20 mL or 25 g/L	Pu(IV) 2.74×10^{-7} M	Natural G. water	8.4	$\sim9.70\times10^4$	~99	1	Lu *et al*. (1998, 2003) Natural groundwater: 0.005 M pH 8.2; TOC 1ppm; Si 30.3 ppm; Na 46;
					$\sim2.1\times10^5$	~99	6	
			Syn-thetic Ground-water	8.6	$\sim2.6\times10^5$	~99	1	
					$\sim2.0\times10^5$	~99	6	

Radio-nuclide	Sorbents	Solution	Ion strength	pH	K_d (mL/g)	Sorp-tion (%)	Equil time (hrs)	Reference / Description
		Pu(V) 2.74×10^{-7} M	Natural Ground-water	8.4	49	55	1	ppm; Ca 13.3 ppm; Mg 1.9 ppm; K 5.4 ppm Aqueous carbonate did not influence the sorption of Pu. Increasing pH from 5.05 to 8.44 increased Pu(V) and had no significant effect on Pu(IV) sorption. Contact time (1, 24, and 96 hr) influenced Pu(V) sorption, but not Pu(IV) sorption. Synthetic groundwater: 0.005 M $Na_2CO_3/NaHCO_3$ The K_d for Pu(IV) were from its Table 4; while the K_d for Pu(V) from its Figure 2 & 3. There are discrepancies in Table 2 and Figure 2 and 3 in the original report.
					93	70	96	
			Syn-thetic Ground-water	8.6	460	92	1	
					~3.96×10^{3}	~99	6	
	Goethite BET 68 m^2/g 0.5 g/20 mL or 25 g/L	Pu(IV) 2.74×10^{-7} M	Natural Ground-water	8.4	~4.1×10^{5}	~99	1	
					~1.5×10^{5}	~99	96	
			Syn-thetic Ground-water	8.6	~2.3×10^{5}	~99	0.5	
					~3.3×10^{5}	~99	96	
		Pu(V) 2.74×10^{-7} M	Natural Ground-water	8.4	120	75	1	
					171	81	96	
			Syn-thetic Ground-water	8.6	1.96×10^{3}	98	1	
					1.96×10^{3}	98	96	
Pu	Hematite <1 µm 0.2 g/L	Pu(V) 2.74×10^{-7} M	Yucca Mt. well J-13 water	8.2	4.9×10^{3}	50	1	Runde *et al*. (2002) Identified $Pu(OH)_4$ and PuO_2 precipitated phases. Increased temperature, decreased Pu solubility.

Powell *et al*. (2004, 2005) investigated the sorption and reduction of Pu(V) onto hematite, goethite and magnetite (containing 10-100 m^2/L iron oxides) over the pH range 3-8 (Figure 2; Table 1). At pH 3, little sorption and reduction of Pu(V) was observed on either hematite (Figure 2A) or goethite (Figure 2B). The sorption rates of Pu(V) onto these iron oxides increase with increasing pH and the extended reaction time. At pH 5-8, the sorption slowly reaches the steady state (~7 days), especially at the lower loadings of hematite, and Pu is essentially 100% removed at pH 8, the overall removal of Pu(V) was found to be approximately second order with respect to hematite concentration. Oxidation state analysis of solutions at approximately neutral pH and 10 m^2/L hematite showed a decrease in the fraction of Pu(V) in the total system (solid + aqueous) with a

corresponding increase in the fraction of Pu(IV) in the total system. In contrast to hematite, Pu(V) sorption to goethite occurs rapidly relative to reduction. At a given pH, the reduction rate is approximately independent of the goethite concentration, although pH has only a slight effect on the overall reaction rate. For magnetite (Figure 2C), at pH 3, the sorption rates are much higher than those for hematite and goethite at the same pH, which may indicate that reduction occurs in the aqueous phase. In the pH range of 5-8, sorption is rate-limiting step, and reduction is mediated by solid phase. The overall reaction was found to be approximately first order with respect to the magnetite concentration and of order -0.34 ± 0.02 with respect to the pH. The Pu(IV) solid phase species become more stable over time.

Goethite, hematite, and magnetite exhibit different sorption kinetics, which is related to the iron content of each mineral. Goethite and hematite are both Fe(III)-bearing minerals and magnetite is a mixed Fe(II/III) mineral. Trace Fe(II) may facilitate the reduction of Pu(V) to Pu(IV). Thus, increasing the Fe(II) content of the system should correlate to an increase in reaction (sorption + reduction) kinetics. This expected trend was confirmed by Hixon *et al*. (2010), who observed a decrease in the rate of Pu(V) reduction to Pu(IV) when the concentration of Fe(II) in SRS sediments was decreased. Therefore, magnetite should exhibit faster kinetics than hematite or goethite. At approximately 50 m^2/L of each mineral and pH 8, kinetic reaction rate for magnetite is an order of magnitude higher than hematite or goethite (Powell *et al*. 2004, 2005).

Sanchez *et al*. (1985) studied the sorption of Pu(IV) and Pu(V) on goethite from $NaNO_3$ (0.1 M) solution that contained 28.5 m^2/L or 0.55 g/L goethite over the pH range of 2-10 (Figure 3; Table 1). The sorption edge of the more strongly hydrolysable Pu(IV) occurs in the pH range of 3 to 5. Pu(IV) sorption onto goethite increases rapidly with increasing pH to approximately pH 6, at which a near-complete sorption and steady state are nearly achieved within 1 hour. Further increase in the equilibration time to 96 hours has little effect on its sorption behavior. An increase in the Pu concentration from 1×10^{-11} M to 1×10^{-10} M results in a slight decrease in sorption percentage from pH 2 to 6, which was not explained, but should not be due to the saturation of surface sites because at 28.5 m^2/L, there are approximately 10^{-4} M sites available for Pu sorption. Therefore, the concentration of surface sites is 6-7 orders of magnitude greater than the Pu concentration. The authors modeled Pu(IV) sorption to goethite using three surface complexes: $\equiv SOPu(OH)_2^{+2}$, $\equiv SOPu(OH)_3^{+}$, and $\equiv SOPu(OH)_4$. This implies the inner-sphere sorption of Pu(IV) to the goethite surface. However, no spectroscopy results are available to confirm these surface species.

Under similar solution conditions, Pu(V) sorption to goethite is different than Pu(IV) sorption to goethite. No sorption is observed below pH 4, sorption increases rapidly with increasing pH. The sorption edge for Pu(V) is the pH 5 to 7, a near complete sorption occurs at approximately pH 8. The sorption edge for Pu(V) shifts to lower pH values with contact time and this appears to be due to the reduction of Pu(V) to Pu(IV) in the presence of goethite surface. These results suggest that redox transformation is likely an important aspect of Pu sorption chemistry and the resulting scavenging of Pu from natural waters. Increasing ionic strength (from 0.1 M to 3 M NaCl or $NaNO_3$ and 0.03 M

to 0.3 M Na_2SO_4) does not influence Pu(V) sorption. In the presence of dissolved organic carbon (DOC), Pu(V) reduction to Pu(IV) occurs in solutions. Pu(IV) sorption on goethite decreased by 30% in the presence of 240 ppm natural DOC. In addition, increasing concentrations of carbonate ligands to 100 meq/L (more specifically total alkalinity) had no effect on Pu(IV) or Pu(V) sorption to goethite. However, above 100 meq/L total alkalinity, the Pu(IV) and Pu(V) sorption on goethite systematically decreased until essentially all Pu was inhibited from sorption, presumably as a result of the formation of a Pu-CO_3 complex (Sanchez *et al*. 1985). As shown in Figure 4, for both Pu(IV) and Pu(V), the carbonate alkalinity at < 100 meg/L shows little effect on the adsorption of Pu onto goethite; however, with further increase in carbonate alkalinity, the adsorption of Pu(IV) and Pu(V) onto goethite significantly decreases until their adsorption become essentially zero at the carbonate alkalinity ~1000 meg/L.

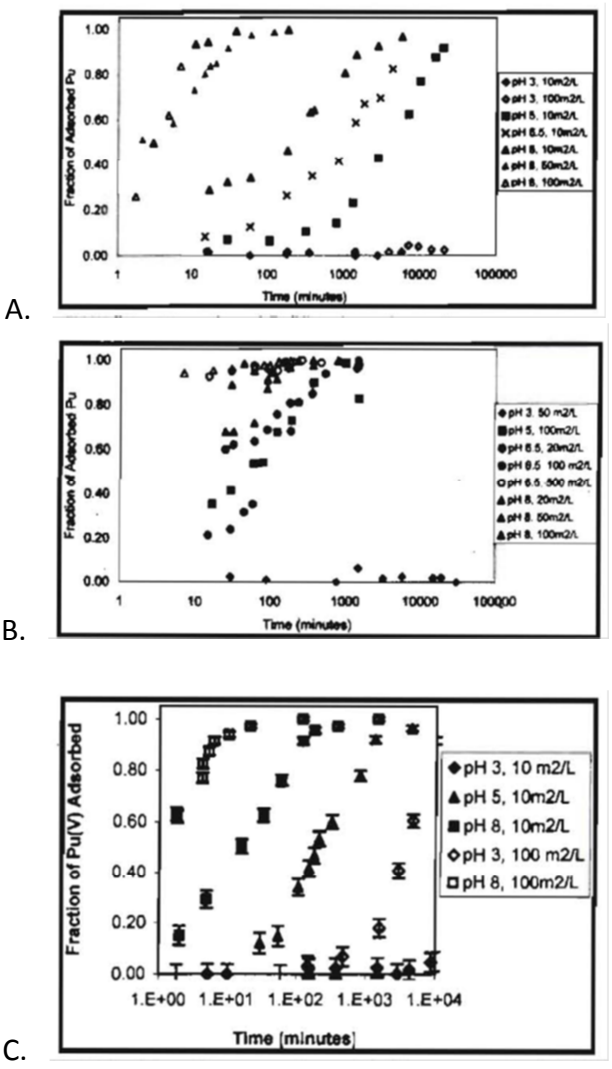

Figure 2. Sorption of Pu(V) on hematite (A), goethite (B) and magnetite (C) at different pH versus time (Powell *et al*. 2004, 2005).

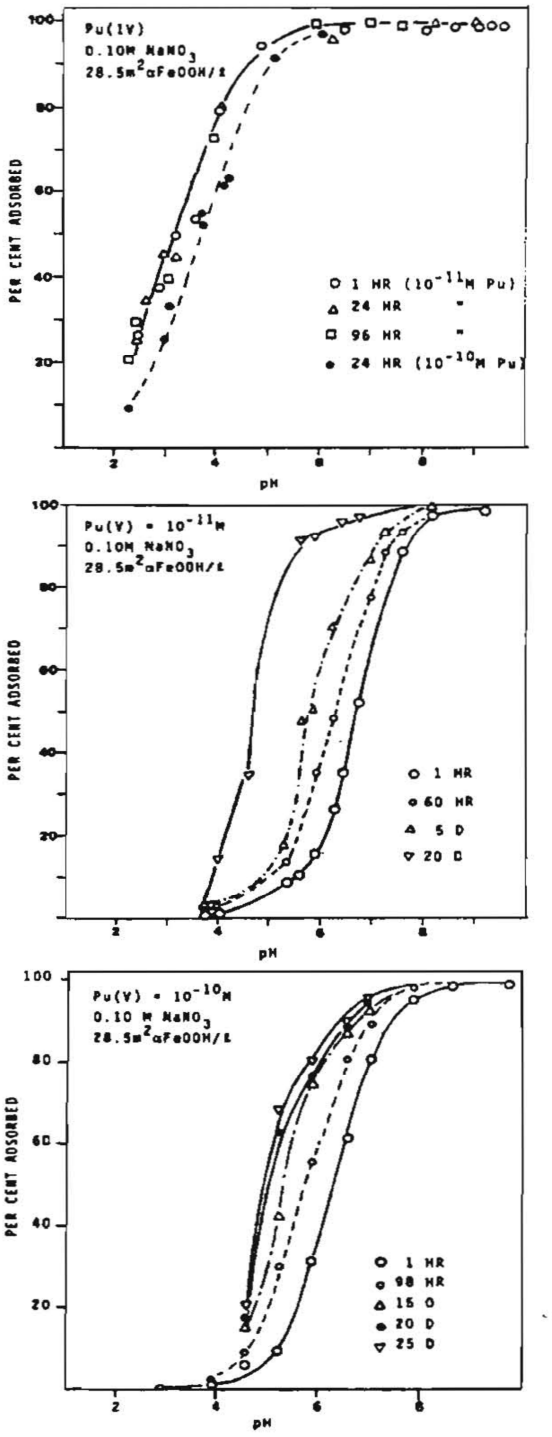

Figure 3. Top) Sorption of Pu(IV) on goethite as a function of pH from 0.1 M $NaNO_3$ solution at two plutonium concentrations (1×10^{-11} and 1×10^{-10} M). Middle) The sorption of Pu(V) on goethite as a function of pH from 0.10 M $NaNO_3$ solution at 1×10^{-11} M. Bottom) Sorption of Pu(V) on goethite as a function of pH from 0.10 M $NaNO_3$ solution at 1×10^{-10} M (Sanchez *et al*. 1985).

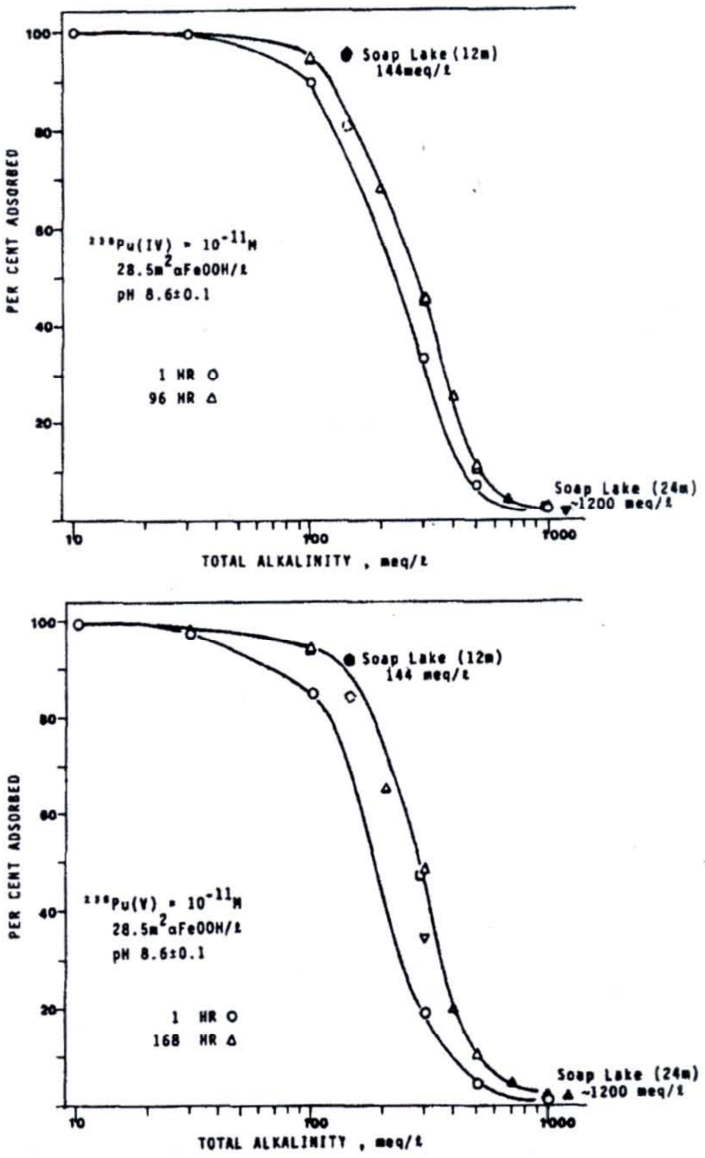

Figure 4. Top) The effect of carbonate alkalinity on the adsorption of Pu(IV) on goethite. Bottom) The effect of carbonate alkalinity on the adsorption of Pu(V) pm goethite. Adsorption from natural Soap Lake water is also shown (solid symbols) (Sanchez *et al*. 1985).

Lu *et al*. (1998, 2003) and Runde *et al*. (2002) studied the sorption of Pu(V) to hematite in Yucca Mountain J-13 well water; a pH 8, Ca and carbonate dominated groundwater as shown in Table 1. Lu *et al*. (1998, 2003) observed that 50-55% of plutonium sorbed immediately after adding Pu(V) to solutions containing 1337.5 m^2/L or 25 g/L colloidal hematite. Over time, the Pu fraction associated with the solid phase slowly increased,

until a steady-state was achieved after ~4 days. Similarly, Runde *et al*. (2002) showed that approximately 45% of plutonium sorbed upon initial mixing, the Pu fraction associated with the solid phases increased with time until a steady-state was reached around 4 days. Approximately 95% of the plutonium was sorbed at a steady-state. The pH of the solutions were not reported over time, but were assumed to be steady at the initial solution pH ~ 8.

Kersting *et al*. (2003) studied the sorption of Pu(V) onto mineral colloids including goethite. The sorption of Pu(V) onto goethite is strong and fast. The initial soluble Pu(V) has ultimately been reduced to the Pu(IV) state on goethite. The mechanism for sorption of Pu(V) on goethite is that the Pu(V) sorbs rapidly, directly on goethite surface as Pu(V) and reduces to Pu(IV) as a result of interaction with goethite surface. Further, XANES spectra showed that Pu(IV) is the dominant oxidation state on goethite when plutonium is added as Pu(V). EXAFS analysis indicated the inner-sphere complexation of Pu(IV) with the goethite surface. Although evidence of plutonium-carbonate complexes exists, there are no Pu-Pu interactions present that would represent precipitation of Pu(IV) on the goethite surface. The sorbed Pu(IV) species likely form edge-sharing bidentate between plutonium and iron octahedra, this means that two oxygen atoms in the Pu hydration sphere are shared with the goethite structure. However, there is no XAS data available in the literature for plutonium sorption to hematite or magnetite.

In addition, Kaplan *et al*. (2006) investigated the influence of pH on Pu desorption / solubilization from SRS sediments in which sand grains and clays are coated with goethite. They found that >99% of the Pu adsorbs onto the sediment within 48 hours, >94% of the aqueous Pu remains as Pu(V), <6% as Pu(VI) and <1% as Pu(IV); in contrast, the adsorbed Pu is exclusively Pu(IV). The fraction of aqueous Pu (Pu_{aq}/Pu_{solid}) decreases by >2 orders of magnitude when the contact time was increased from 1 to 33 days, presumably the result of Pu(V) reduction to Pu(IV). After desorption, 96% of the Pu_{aq} is Pu(V/VI). The Pu_{aq} concentrations from the desorption experiment are similar to those of the Pu(V) amended sorption studies that were permitted to equilibrate for 33 days, suggesting that the latter had reached steady state. The Pu_{aq} concentrations as a function of pH follows near identical trends with literature solubility values for PuO_2(am), except that the desorption values are lower by over an order of magnitude, indicating that pH has a more pronounced effect on solubility and Pu_{aq} concentrations than on sediment charge density (or Pu_{aq} oxidation state distribution). Slight changes in system pH can have a large impact on Pu solubility and the tendency of Pu to sorb to sediment, thereby influencing Pu subsurface mobility. Hixon *et al.* also studied the influence of iron redox transformations on Pu sorption to SRS sediments and found that native Fe(II) in the sediments is responsible for the reduction of trace level Pu in the systems, in agreement with the iron oxide surface-mediated reduction mechanism of Pu(V) (Powell *et al*. 2004, 2005) and Pu(VI) (Romanchuk *et al*. 2011).

3.2 Uranium

A summary of the uranium sorption information (adsorption coefficient K_d, adsorption percentage, initial Pu concentration, pH, ion strength, equilibrium time, and sorbent loading) to iron oxyhydroxide phases is given in Table 2.

There are more references related to uranium than plutonium sorption to oxyhydroxides (hematite, magnetite, goethite and ferrihydrites) as shown in Table 2. In CO_2 or carbonate ligand free systems, uranyl (UO_2^{2+}), monodentate (as UO_2OH^+) and bi- or tri-dendate (as $UO_2(OH)_2^0$ and $UO_2(OH)_3^-$) are chief complexation species with increasing pH as shown in Figure 5 (Missana *et al*. 2003), although the detailed speciation may be slightly different from different model calculations (Hsi and Langmuir 1985 and Missana *et al*. 2003). As shown in Figure 6, the sorption profiles of U onto these iron oxyhydroxides are generally similar and form S-type (or sigmoidal type) sorption edges at the pH range of 2-10. The sorption is very little or near zero at pH <3, the sorption increases dramatically with increasing pH, a near complete sorption of U is normally achieved at the pH 5-6 and remains until pH 10 studied (Hsi and Langmuir 1985, Waite *et al*. 1994, Payne *et al*. 1998, Missana *et al*. 2003, Tao *et al*. 2004, Zeng *et al*. 2009). In Figure 6, the sorption profiles of U onto synthetic and natural hematite are slightly different from those for ferric hydroxide and goethite. This difference is probably due to the limited surface area, particle sizes and thus the limited available sorption sites of the hematite sorbents (Missana *et al*. 2003, Zeng *et al*. 2009). Ca and Mg at 10^{-3} M do not significantly affect uranyl sorption (Hsi and Langmuir 1985), while the ion strength change of $NaNO_3$ from 0.1 M to 0.001 M appears to have little influence on the sorption profiles of U onto iron oxides and hydroxides (Missana *et al*. 2003). In addition, the sorption of U onto iron oxides and hydroxides are fast and normally reach the steady state within 48 hours, and the sorption profiles are similar with the extended contact time up to 3 months (Missana *et al.* 2003). Mahoney *et al*. (2008) re-evaluated uranyl sorption onto hydrous ferric oxide using the diffuse layer model database.

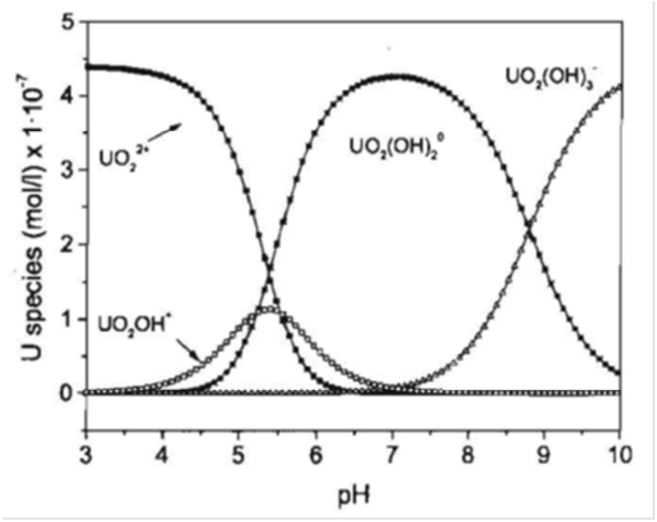

Figure 5. Aqueous speciation of uranium at I = 0.1 M $NaNO_3$ and [U] = 4.4×10^{-7} M. Major species are shown only (Missana *et al.* 2003).

Table 2. Uranium sorption to iron oxyhydroxide phases

Radio-nuclide	Sorbents	Solution	Ion strength	pH	K_d (mL/g)	Sorption (%)	Equil time (hrs)	Reference / Description
U	Ferri-hydrite 0.0005 M or 0.084 g/L	U 1×10^{-6} M P_{CO2} $10^{-3.5}$ bar	0.1 M $NaNO_3$	3.5	120	1	48	Hiemstra *et al*. (2009) The sorption profiles against pH are similar with (1) the initial U conc. from 0.01 to 100 μM, (2) with ion strength from 0.004 M to 0.5 M, and (3) ferrihydrite loading from 0.0005 M to 0.01 M. The influence of carbonate complexes and high pH on uranium sorption is far more pronounced than with Pu.
				5.5	5.83×10^{5}	98		
				8.2	2.26×10^{5}	95		
				10	0	0		
		U 1×10^{-6} M P_{CO2} 0.01 bar	0.1 M $NaNO_3$	3.0	120	1	48	
				5.2	5.83×10^{5}	98		
				6.8	1.18×10^{6}	99		
				7.8	0	0		
U	Hematite 12 nm 1 g/L	U 1×10^{-6} M	0.01 M $NaNO_3$	3.0	149	13	48	Zeng *et al*. (2009) U Sorption onto colloidal hematite decreases and the sorption edge shifts toward higher pH as the particle size increased from 12 to 125 nm. However, the coordination environments of adsorbed U(VI) species are not significantly different on hematite of different sizes.
				3.5	2.13×10^{3}	68		
				4.1	$\sim9.9\times10^{4}$	~99		
				10.2	$\sim9.9\times10^{4}$	~99		
	Hematite 70 nm 1 g/L	U 1×10^{-6} M	0.01 M $NaNO_3$	3.0	0	0	48	
				4.2	177	15		
				5.0	1.5×10^{3}	60		
				5.8	$\sim9.9\times10^{4}$	~99		
				9.9	$\sim9.9\times10^{4}$	~99		
	Hematite 12 nm 1 g/L	U 1×10^{-4} M	0.01 M $NaNO_3$	3.0	64	6	48	
				4.0	667	40		
				4.5	7.33×10^{3}	88		
				5.8	$\sim9.90\times10^{4}$	~99		
				10.2	$\sim9.9\times10^{4}$	~99		
	Hematite	U	0.01 M	4.0	0	0	48	

Radio-nuclide	Sorbents	Solution	Ion strength	pH	K_d (mL/g)	Sorption (%)	Equil time (hrs)	Reference / Description
	70 nm 1 g/L	1×10^{-4} M	$NaNO_3$	5.2	471	32		
				6.9	3.0×10^{3}	75		
				10.1	1.08×10^{3}	52		
U	Goethite 0.09 g/L	U 1×10^{-5} M P_{CO2} $10^{-3.5}$ bar	0.09 M $NaNO_3$	3.4	0	0	24	Sherman *et al*. (2008) The dominant surface complex in CO_2-free systems is a bidentate corner-sharing complex $(\equiv FeOH)_2UO_2(H_2O)_3$. Which can form on the dominant {101}. In the presence of CO_2, UO_2 sorption at lower pH is enhanced due to the formation of a $(\equiv FeO)CO_2UO_2$ ternary complex. With pH increase, U(VI) desorbs by the formation of aqueous carbonate and hydroxyl complexes. This desorption is preceded by the formation of a second ternary surface complex $(\equiv FeOH)_2UO_2CO_3$.
				6.5	1.0×10^{5}	90		
				9.5	0	0		
		U 1×10^{-6} M P_{CO2} $10^{-3.5}$ bar	0.09 M $NaNO_3$	3.5	463	4	24	
				5.5	2.67×10^{5}	96		
				8.0	8.15×10^{4}	88		
				9.5	0	0		
		U 1×10^{-7} M P_{CO2} $10^{-3.5}$ bar	0.09 M $NaNO_3$	3.5	1.96×10^{3}	15	24	
				5.0	~1.1×10^{6}	~99		
				8.0	~1.1×10^{6}	~99		
				9.5	0	0		
		U 1×10^{-5} M P_{CO2} < 10^{-6} bar	0.09 M $NaNO_3$	4.2	0	0	48	
				7.5	2.11×10^{5}	95		
				10	5.44×10^{5}	98		
		U 1×10^{-6} M P_{CO2} < 10^{-6} bar	0.09 M $NaNO_3$	3.5	0	0	48	
				6.2	5.44×10^{5}	98		
				9.9	2.67×10^{5}	96		
		U 1×10^{-7} M P_{CO2} < 10^{-6} bar	0.09 M $NaNO_3$	3.5	0	0	48	
				5.5	~1.1×10^{6}	~99		
				9.9	~1.1×10^{6}	~99		
U	Hematite 10 g/L	UO_2^{2+} 3.2×10^{-5} M	0.1 M $NaNO_3$	4	2.0	2	36	Tao *et al*. (2004) The UO_2^{2+} sorption edge occurs at pH 5-6. With ion strength increase, the sorption edge shifts toward higher pH and become broader.
				5.3	25	20		
				5.5	67	40		
				6.0	669	87		
				8	567	85		
				11	1.33×10^{3}	93		
	Hematite 10 g/L	UO_2^{2+} 3.2×10^{-5} M	0.01 M $NaNO_3$	3.2	3	3	36	
				5.5	25	20		
				5.8	100	50		

Radio-nuclide	Sorbents	Solution	Ion strength	pH	K_d (mL/g)	Sorption (%)	Equil time (hrs)	Reference / Description
				7.2	1.33×10^3	93		
				10.2	1.9×10^3	95		
	Hematite 10 g/L	UO_2^{2+} 3.2×10^{-5} M	0.001 M $NaNO_3$	4.4	4	4	36	
				6.0	67	40		
				7.3	488	83		
				9.1	1.33×10^3	93		
U	Goethite 2 g/L	U 4.4×10^{-7} M O_2, CO_2-free	0.1 M $NaClO_4$	3.3	0	0	360	Missana *et al*. (2003) Profiles are same for 15 days and 3 months; shift slightly to lower pH with ion strength change to 0.001 M, to higher pH with goethite loading to 0.16 g/L.
				3.8	81	14		
				4.8	2.83×10^3	85		
				5.8	~4.95×10^4	~99		
				10.5	~4.95×10^4	~99		
U	Hematite BET 32.8 m^2/g 0.2 g/L	U 1×10^{-6} M P_{CO2} $1\times10^{-3.5}$ bar	0.1 M $NaNO_3$	4.0	1.1×10^3	18	24	Bargar et al. (2000) Dimeric hematite-U(VI)-carbonate ternary complexes are identified.
				4.0	1.49×10^3	23	120	
				8.9	1.94×10^3	28	24	
				8.9	2.58×10^3	34	120	
U	Biogenic Fe oxide Fe 3.92 moles per kg solids	U 6×10^{-5} M	Ground water with Cs, Sr, Pb, U, others	8.3	4.37×10^3		48	Ferris *et al*. (2000) Bacteriogenic Fe oxides are amorphous hydrous ferric oxide and ferrous iron oxidizing bacteria. K_d decreased with the mass fraction of reducible oxide, implying that metal uptake is strongly influenced by bacterial organic matter.
	Biogenic Fe oxide Fe 6.63 moles per kg solids	U 6×10^{-5} M		8.3	5.5×10^3		48	
	Biogenic Fe oxide Fe 5.29 moles per kg solids	U 4.5×10^{-5} M		8.3	2.14×10^3		48	
	Biogenic Fe oxide Fe 7.64 moles per kg solids	U 4.5×10^{-5} M		8.3	1.78×10^3		48	
U	Goethite 10 g/L	U 2×10^{-6} M		3.7	~9.9×10^3	~99	24	Moyes *et al.* (2000)

Radio-nuclide	Sorbents	Solution	Ion strength	pH	K_d (mL/g)	Sorption (%)	Equil time (hrs)	Reference / Description
		U 4×10^{-6} M		3.7	400	80		On both iron hydroxides uranium uptake occurs by surface complexation and ceases when the surface is saturated. Bidentate inner-sphere surface complexes are formed by coordination of two surface oxygens from the iron octahedron in the equatorial plane of the complex.
		U 1×10^{-5} M		3.7	67	40		
	Lepido-crocite 10 g/L	U 2×10^{-6} M		3.6-4.8	~9.9×10^{3}	~99	24	
		U 6×10^{-6} M		3.6-4.8	~9.9×10^{3}	~99		
		U 1.2×10^{-5} M		3.6-4.8	100	50		
		U 3×10^{-5} M		3.6-4.8	30	23		
U	Hematite 0.53 g/L	U 5×10^{-7} M CO_2 free	0.1 M $NaNO_3$	4.3	596	24	48	Liger *et al*. (1999) ≡Fe-UO_2OH is the major sorption species.
				5.0	7.6×10^{3}	82		
				5.6	6.1×10^{4}	97		
				7.7	~1.87×10^{5}	~99		
U	Ferri-hydrite 600 m^2/g 0.084 g/L	U 1×10^{-6} M P_{CO2} $1\times10^{-3.5}$ bar	0.1 M $NaNO_3$	3	118	1	48	Payne *et al*. (1998) Waite *et al*. (1994) To increase ferrihydrite loading to 1.68 g/L, the profile becomes broader on both pH side. To increase P_{CO2} to 0.01 bar, the higher pH side of profile shifts toward lower pH. To increase ion strength, the profile shifts to lower pH. To add 9 mg/L humic acid, the profile becomes slightly broader.
				4.6	1.58×10^{4}	57		
				5.4	3.85×10^{5}	97		
				8.2	2.26×10^{5}	95		
				10	0	0		
	Ferrihydrite 600 m^2/g 0.084 g/L	U 1×10^{-4} M P_{CO2} $1\times10^{-3.5}$ bar	0.1 M $NaNO_3$	4	0	0	48	
				5	9.74×10^{3}	45		
				5.5	4.22×10^{4}	78		
				6.5	2.86×10^{5}	96		
				7.5	8.73×10^{4}	88		
				8	5.1×10^{3}	30		
				8.8	0	0		
U	Ferri-hydrite BET 306	U 1×10^{-5} M CO_2 free	0.1 M $NaNO_3$	3	110	10	No data	Hsi and Langmuir (1985)
				5.2	~9.9×10^{4}	~99		

Radio-nuclide	Sorbents	Solution	Ion strength	pH	K_d (mL/g)	Sorption (%)	Equil time (hrs)	Reference / Description
	m^2/g 1 g/L			8.8	~9.9×10^4	~99		Ca and Mg at 10^{-3} M did not significantly affect uranyl sorption. Uranyl carbonate and hydrocarbonate severely inhibited uranyl sorption. In carbonate free solution, monodentate UO_2OH^+ and mono-, bi- or tri-dendate $(UO_2)_3OH^+$ are chief complexation species. It was necessary to slightly vary the intrinsic constants for sorption of the di- and tri-carbonate complexes to fit the uranyl sorption data at total carbonate concentration of 10^{-2} and 10^{-3} M.
	Goethite BET 45 m^2/g 1 g/L	U 1×10^{-5} M CO_2 free	0.1 M $NaNO_3$	3.6	220	18		
				5.6	2.4×10^4	96		
				9.0	~9.9×10^4	~99		
	Synthetic hematite BET 3.1 m^2/g 1 g/L	U 1×10^{-5} M CO_2 free	0.1 M $NaNO_3$	4.1	0	0		
				5.0	667	40		
				6.6	1.5×10^3	60		
				9.4	4.9×10^4	98		
	Natural hematite BET 1.8 m^2/g 1 g/L	U 1×10^{-5} M CO_2 free	0.1 M $NaNO_3$	5	0	0		
				5.5	250	20		
				7	3.0×10^3	75		
				9.5	1.63×10^3	62		
	Goethite BET 45 m^2/g 1 g/L	U 1×10^{-5} M CO_2 free 0.001 M $NaHCO_3$	0.1 M $NaNO_3$	3.9	250	20		
				5.4	~9.9×10^4	~99		
				8.5	4.9×10^4	98		
	Goethite BET 45 m^2/g 1 g/L	U 1×10^{-5} M CO_2 free 0.01 M $NaHCO_3$	0.1 M $NaNO_3$	4.3	2.33×10^3	70		

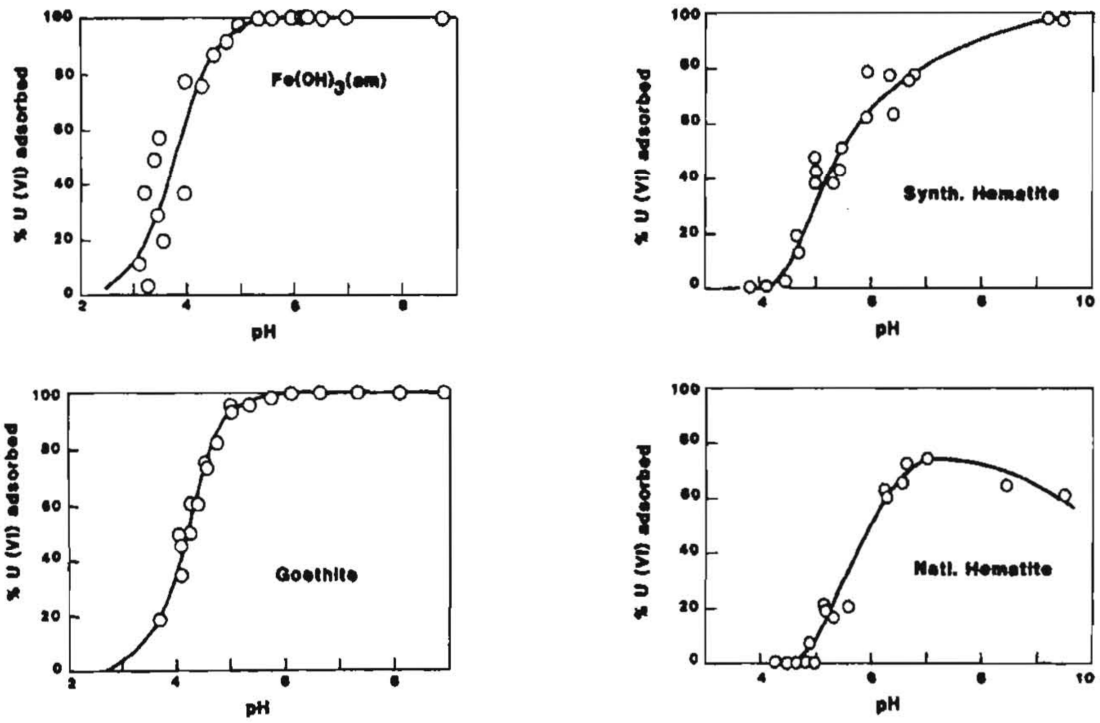

Figure 6. Sorption of uranyl versus pH at $\sum U = 1\times10^{-5}$ M onto 1 g/L suspension of ferri- hydroxide (left top), goethite (left bottom), synthetic hematite (right upper) and natural hematite (right bottom) in 0.1 M $NaNO_3$ solutions at 25 °C. Symbols denote the experimental data, the solids curves are model calculated assume the given surface parameters and monodendate surface complexes of UO_2OH^+ and $(UO_2)_3(OH)_5^+$ with p*Kins values of 8.0 and 15.0, respectively (Hsi and Langmuir 1985).

EXAFS studies indicated that the uranyl and hydrolyzed uranyl species form mononuclear bidentate complex ($\equiv Fe(OH)_2UO_2(H_2O)_n$ or E2 complex) with iron oxides and hydroxides, the two oxygen atoms of the distorted U-O octahedral are shared with the Fe-O octahedron on the surface (Figure 11a, also Waite *et al*. 1994, Reich *et al*. 1998), while at higher pH or higher initial U concentration, the U species can form multiple-nuclear polymerization or precipitates. However, more recently, Sherman *et al.* (2008) studied surface complexation of U(VI) on goethite (α-FeOOH). They argued that the previously proposed E2 complex, bidentate $\equiv Fe(OH)_2UO_2(H_2O)_n$ complex, can only form on the {210} or {010} surface which comprise only small fraction (~1%) of goethite surface area. The U-Fe distance attributed previously to the E2 complex in EXAFS spectra can be fitted entirely by multiple scattering. At the same time, the effect of multiple scattering is to mask their proposed C2 complex (bidentate corner-sharing complex $(\equiv FeOH)_2UO_2(H_2O)_3$). Therefore, they proposed that the dominant surface complex in CO_2-free systems is a C2, which can form on the dominant {101} surface (Figure 7).

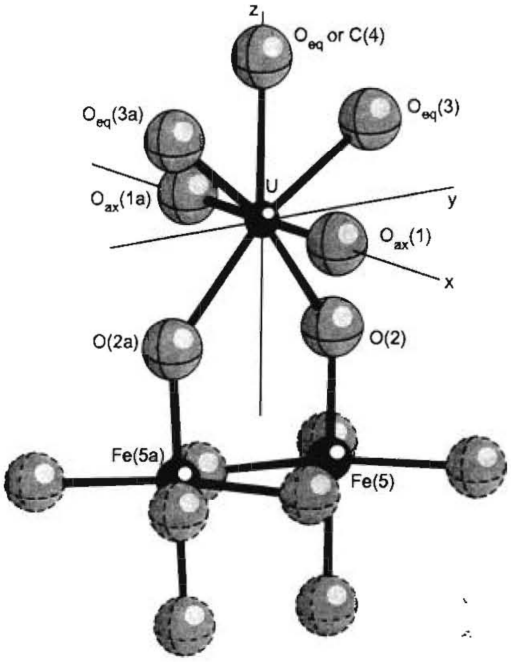

Figure 7. Cluster used in EXAFS fits for U(VI) sorbed to goethite (Sherman *et al.* 2008).

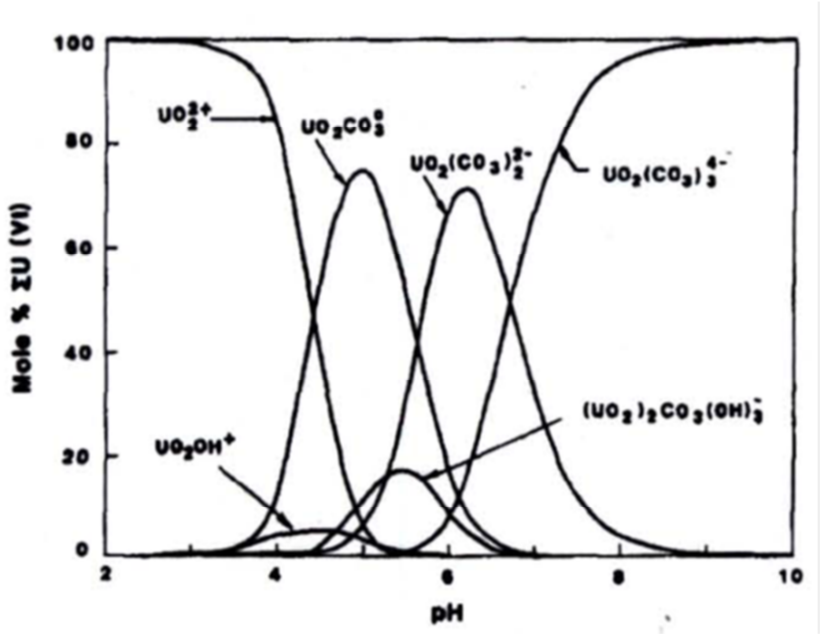

Figure 8. Distribution of uranyl-hydroxyl and carbonate complexes versus pH at $\sum U = 1 \times 10^{-5}$ M, total carbonate 0.01 M in 0.1 M $NaNO_3$ solutions at 25 °C (Hsi and Langmuir 1985).

In the systems with CO_2 or carbonate ligand, uranyl carbonate and hydrocarbonate complexes occur at pH 4 and become dominant at higher pH (Figure 8), although the actual U complexes may be slightly different from different model calculations (Hsi and Langmuir 1985, Waite *et al*. 1998, Payne 1999, Sherman *et al*. 2008, Payne *et al*. 2011). It was necessary to slightly vary the intrinsic constants for sorption of the di- and tri-carbonate complexes to fit the uranyl sorption data at a total carbonate concentration of 10^{-2} and 10^{-3} M (Hsi and Langmuir 1985).

In the systems with CO_2 or carbonate ligands, the sorption of U onto ferrihydrite and other iron oxides / hydroxides are fairly similar (Hsi and Langmuir 1985, Waite *et al*. 1998, Payne 1999, Bargar *et al*. 2000, Sherman *et al*. 2008, Hiemstra *et al.* 2009, Rossberg *et al*. 2009). As shown in Figure 9, the sorption of uranyl onto ferrihydrite is strongly dependent on pH. At pH < 4, the sorption of U is very low, but the sorption of U onto iron oxides and hydroxides increases sharply with pH, the complete sorption is seen at pH ~5 until pH 8, the sorption of U onto ferrihydrite decreases sharply starting from pH 8, and essentially becomes non-existent at pH >9. This differs greatly from Pu, where at pH 9.8, plutonium sorption appears to be strong (Santchez *et al*. 1985) when the carbonate alkalinity is <100 meq/L. With an increase in the initial U(VI) concentration from 1×10^{-8} M to 1×10^{-4} M (Figure 9, left upper), the sorption profiles are similar, but the left-side edge shift slightly toward higher pH and the right-side edge to lower pH. With an increase in the sorbent loading from 0.001 M Fe or 0.084 g/L ferrihydrite to 0.02 M Fe or 1.68 g/L (Figure 9, left bottom), the left-side edge slightly shifts to lower pH, and the right-side edge to higher pH. The sorption of U(VI) shows little change with the ion strength from 0.004 M to 0.5 M $NaNO_3$ (Figure 9, right upper). However, with CO_2 partial pressure increase from $1\times10^{-3.5}$ bar to 0.02 bar, the right-side edge shifts toward lower pH (Figure 9, right bottom) (Hiemstra *et al*. 2009, Waite *et al*. 1998, Payne 1999).

The uranyl carbonate and hydrocarbonate complexes severely inhibit uranyl sorption onto iron oxides and hydroxides (Hsi and Langmuir 1985). Duff and Amrhein (1996) also suggested that U(VI)-carbonate ternary complexes should adsorb weakly on goethite. Hiemstra *et al.* proposed that in the presence of carbonates, the total concentration of U(VI) in solutions may increase as a result of desorption. This is more clearly seen at high pH. Desorption is mainly due to the formation of dissolved uranyl-carbonate complexes such as $UO_2CO_3^0$ (aq), $UO_2(CO_3)_2^{2-}$ (aq) and $UO_2(CO_3)_3^{4-}$ (aq). Desorption of uranyl is counteracted by the sorption of carbonate ions to the ferrihydrite surface. The coordination environment of the ferrihydrite surface may limit the complexity of U(VI) surface speciation in comparison to that observed in aqueous solution. Binding of 1:1 uranyl-carbonate complex at the surface is suggested from the results of batch sorption study and associated surface complexation modeling; however, coordination of U(VI) with two or more carbonate ligands may prevent surface coordination (Waite *et al*. 1994).

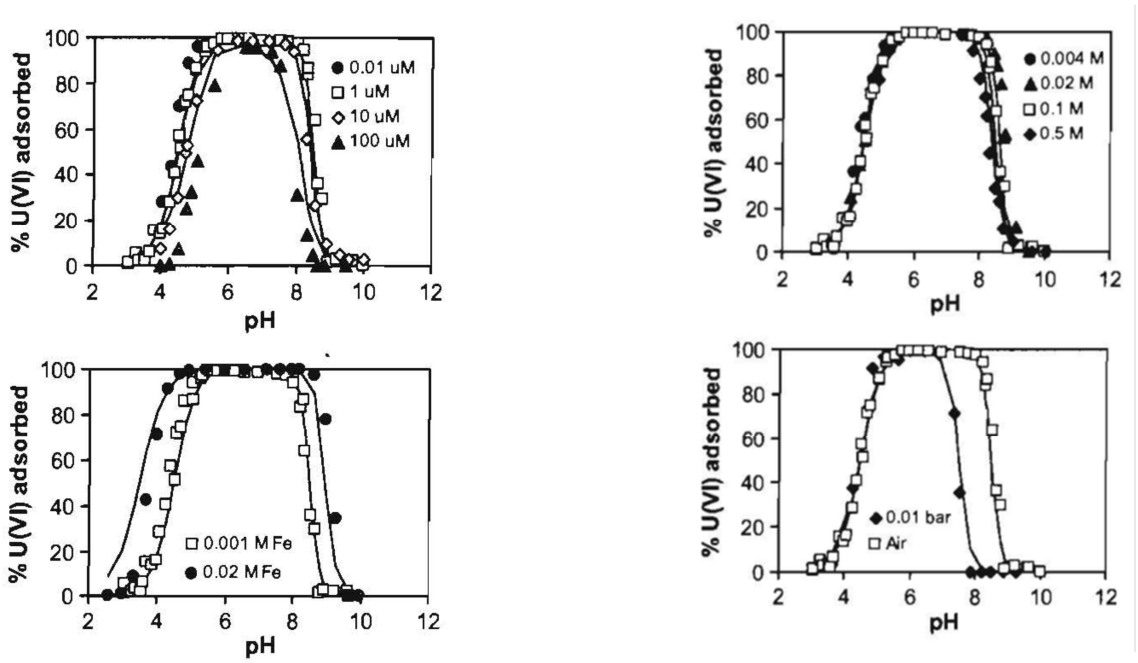

Figure 9. The fraction of uranyl adsorbed to ferrihydrite as a function of pH from 2 to 10 in the open systems. All systems are based on 1×10^{-3} M Fe or 0.084 g/L ferrihydrite, $P_{CO2} = 10^{-3.5}$ bar, and an initial U(V) concentration of 1×10^{-6} M, unless otherwise indicated in the figures. The sorption of U onto ferihydrite with (1) initial U concnetration (left upper), (2) ferrihydrite loading (left bottom), (3) ion strength of $NaNO_3$ (right upper), and (4) CO_2 partial pressure (right bottom) (Payne *et al.* 1998, Payne 1999, Hiemstra *et al.* 2009).

However, Bargar *et al.* (2000) measured U(VI) sorption on hematite using EXAFS spectroscopy and electrophoresis under conditions relevant to surface waters and aquifers (0.01 to 10 mM dissolved uranium concentrations, in equilibrium with air, pH 4.5 to 8.5). Both techniques suggest the existence of anionic U(VI)-carbonato ternary complexes. Computational modeling of the EXAFS portion of the spectra indicate that U(VI) is simultaneously coordinated to surface FeO_6 octahedra and carbonate (or bicarbonate) ligands in bidentate fashions. The ternary complexes have an inner-sphere metal bridging (hematite-U(VI)-carbonato) structure (Figure 10). About ≥50% of adsorbed U(VI) is comprised of monomeric hematite-U(VI)-carbonato ternary complexes, even at pH 4.5. Multimeric U(VI) species were observed at pH ≥ 6.5 and aqueous U(VI) concentrations approximately an order of magnitude more dilute than the solubility of crystalline β-$UO_2(OH)_2$. Based on structural constraints, these complexes were interpreted as dimeric hematite-U(VI)-carbonato ternary complexes. These results suggest that Fe-oxide-U(VI)-carbonato complexes are likely to be important transport-limiting species in oxic aquifers throughout a wide range of pH values.

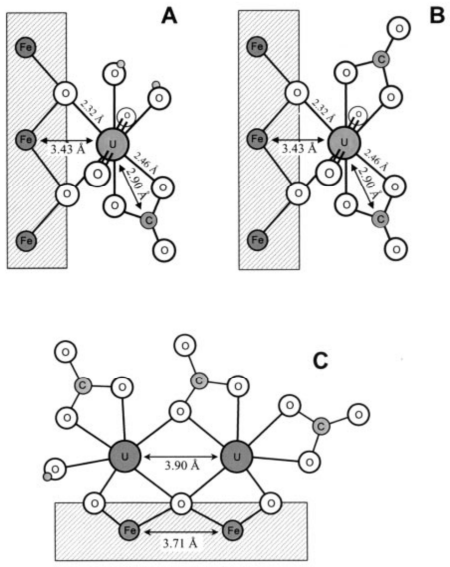

Figure 10. Structural models for postulated ≡$Fe(OH)_2(UO_2)(OH, H_2O)_{4-2t}(CO_3)_t$ complexes on hematite. (A) t=1, (B) t=2, (C) proposed dimeric ≡$Fe_2O_3(UO_2)_2(OH, H_2O)_{7-2t}(CO_3)_t$ bonded to edge-sharing FeO_6 octahedra. To illustrate the dimension mismatch between the multimeric complexes and hematite, Fe atoms are shown with the maximum Fe-Fe separation found in hematite for neighboring FeO_6 octahedra (Bargar *et al*. 2000).

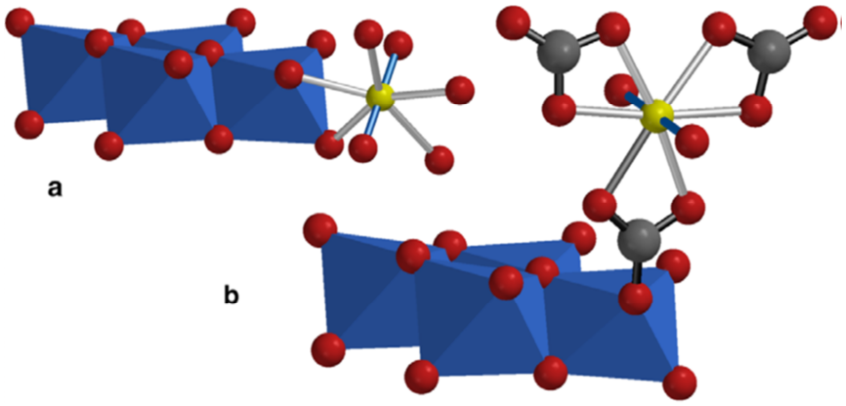

Figure 11. Representation of the most prominent uranyl surface complexes in open systems. (a) Uranyl bound by two singly-coordinated surface group present at a free edge. For this geometry with d(Fe-U) = 3.45 Å and d(U-O_{edge}) = 2.49 Å, d(O-O)$_{edge}$ is 2.87 Å. The outer ligand of the uranyl surface complex in (a) may be OH, OH_2, or CO_3 (not shown). (b) A uranyl tris-carbonate complex that is singly-coordinated to a Fe ion in the solid via a carbonate group (Hiemstra *et al.* 2009, Rossberg *et al*. 2009).

More recently, Rossberg *et al.* (2009) and Hiemstra *et al*. (2009) reinvestigated the identity and structural coordination of uranyl sorption complexes onto ferrihydrite in a range of conditions (pH, CO_2 partial pressure, ionic strength, U(VI) concentration, and ferrihydrite loading) using a combination of U L_{III}-edge extended X-ray absorption fine structure (EXAFS) spectroscopy and iterative transformation factor analysis. They found that their results can only be quantified and explained by two structurally different types of uranyl surface complexes (Figure 11): (1) a binary uranyl surface complex with a bidentate coordination to edges of $Fe(O,OH)_6$ octahedra and (2) a uranyl tris-carbonato surface complex ($\equiv(UO_2)(CO_3)_3^{4-}$) where one carbonate ion bridges uranyl to the surface. Both surface complexes agree qualitatively and quantitatively with predictions by a charge distribution (CD) model. The first uranyl surface complex has equatorial ligands ($-OH_2$, -OH, or one $-CO_3$ group) that point away from the surface, and the uranyl complex is directly attached to surface atoms by edge-sharing with $Fe(O,OH)_6$ octahedron on ferrihydrite surface. The second uranyl-tri-carbonate complex forms monodentate surface complex through one CO_3 group to bridge uranyl and ferrihydrite surface. This species is most abundant in systems with a high pH and carbonate concentration. At these conditions, however, it is responsible for significant uranyl sorption, whereas standard models would predict only weak sorption, which has significant implications for immobilization of uranyl in carbonate-rich aqueous environments. At high uranyl concentrations, uranyl polymerizes at the surface of ferrihydrite giving, for instance, tris-uranyl surface complexes with and without carbonate.

Steward *et al*. (2010) studied and quantified the influence of Ca and carbonate on the impact of uranyl speciation and on the sorption of U onto goethite. Calcium and carbonate were introduced into the solution system containing U and goethite at defined levels to provide a range of aqueous uranyl species. U(VI) sorption is directly linked to UO_2^{2+} speciation, with the extent of retention decreasing with formation of ternary uranyl-calcium-carbonate species. Sorption isotherms under conditions studied are linear, and K_d values decrease from 48 to 17 L/kg for goethite as Ca concentration increases from 0 to 1 mM at pH 7. These observations reveal that, in carbonate-bearing waters, neutral to slightly acidic pH values (~5) and limited dissolved calcium are optimal for uranium sorption. Steward *et al*. (2011) further investigated the impact of U(VI) speciation on the extent and rate of reduction, with specific emphasis on the effect of dissolved Ca, and the impact of Fe(III) (hydr)oxides (ferrihydrite, goethite and hematite) on reduction. The amount of U removed from solution during 100 h of incubation with *S. putrefaciens* is 77% with no Ca or ferrihydrite present, but only 24% (with ferrihydrite) and 14% (no ferrihydrite) are removed for systems with 0.8 mM Ca. Goethite and hematite decrease the dissolved Ca concentration through sorption and thus tend to diminish the effect of Ca on uranium reduction. They revealed the predominant influence of uranyl speciation, specifically the formation of uranyl-calcium-carbonate complexes, and ferrihydrite on the rate and extent of U reduction in complex geochemical systems.

In addition, Duff *et al*. (2002) studied uranium co-precipitation with iron oxide minerals in solutions of U(VI) and Fe(III). They found that U(VI) is incorporated in the Fe oxide as urinate (without axial O atoms) until a point of saturation is reached. Beyond this

excess in U concentration, precipitating U(VI) forms discrete crystalline uranyl phases that resemble the uranyl oxide hydrate schoepite [$UO_2(OH)_2 \cdot 2H_2O$]. Nico *et al*. (2009) studied the form of solid phase U after Fe(II) induced anaerobic remineralization of ferrihydrite in the presence of aqueous and absorbed U(VI) under both abiotic batch and biotic flow conditions. In synthetic ground waters containing 0.168 mM U(VI), 3.8 mM carbonate, and 3.0 mM Ca^{2+}, in spite of the high solubility of U(VI) under these conditions, appreciable removal of U(VI) from solution was observed in both the abiotic and biotic systems. The majority of the removed U was determined to be substituted as oxidized U (U(VI) or U(V)) into the octahedral position of the goethite and magnetite formed during ferrihydrite remineralization. The produced solids were shown to be resistant to both extraction (30 mM $KHCO_3$) and oxidation (air for 5 days), suggesting the potential importance of sequestration in Fe oxides as a stable and immobile form of U in the environment.

Aamrani *et al*. (2007) studied the sorption of U onto magnetite as a main product of anoxic steel corrosion using X-ray photo electron spectroscopy (XPS) and extended X-ray absorption spectroscopy (XAS). They did not specify the sorption percentage or K_d of U on magnetite although a high sorption was expected. However, the EXAFS results indicated that the magnetite samples with U sorption has characteristics of both UO_2 and schoepite, and U species adsorbed onto magnetite would be a mixture of U(VI) and U(IV). Duro *et al*. (2008) found that under anoxic conditions, U(VI) is adsorbed onto magnetite surface, whereas under reducing conditions at different H_2 (g) pressures, U is present in tetravalent form as amorphous UO_2.

Rovira *et al*. (2007) further investigated the influence of the steel corrosion products on the radionuclides released from the fuel. In this study, steel coupons were reacted to form magnetite on their surfaces by anaerobic steel corrosion in an autoclave reactor at an overpressure of 8 atmosphere of H_2 (g). The corroded steel coupons, which were confirmed to form magnetite on their surfaces by X-ray diffraction, were contacted with a U(VI) solution at two different H_2 (g) pressures (1 and 7.6 atmospheres). The U concentrations in the solutions were monitored and determined, and the compositions of the coupons were studied at the end of this experiment. They concluded that magnetite generated on steel coupons is able to not only retain U as a sorption, but also reduce U(VI) to U(IV) to a higher extent than commercial magnetite, thus providing an effective retardation path to the migration of uranium (and, potentially, other actinides) out of repository

3.3 Neptunium

A summary of the neptunium sorption information (adsorption coefficient K_d, adsorption percentage, initial Pu concentration, pH, ion strength, equilibrium time, and sorbent loading) to iron oxyhydroxide phases is given in Table 3.

In the solution systems containing Np(V) 4.5×10^{-13} to 4.5×10^{-11} M and 0.1 M $NaNO_3$ at 25 °C, little Np(V) sorbs onto ferrihydrite at pH ≤4.5 (Table 3). Above that pH, Np sorption onto ferrihydrite increases gradually with increasing pH until pH 8, Np(V) is

almost completely sorbed by ferrihydrite at pH 8-10 (Girvin *et al*. 1991). The S-type sorption edge shifts toward lower pH with an increase in the ferrihydrite loading. The dominant aqueous NpO_2^+ sorbes onto ferrihydrite surface to form $NpO_2(OH)^0$ surface complex. In natural groundwater systems like Yucca Mountain J-13 well waters, Np(V) sorption onto hematite (< 1 μm) at 0.2 g/L is fairly low at pH ~8 and its kinetic reaction is also slow (Runde *et al*. 2002), although another report indicated that Np(V) incrementally but steadily sorbs onto hematite at pH from 5 to 10 (Jain *et al*. 2007).

Table 3. Neptunium sorption to iron oxyhydroxide phases

Radio-nuclide	Sorbents	Solution	Ion strength	pH	K_d (mL/g)	Sorp-tion (%)	Equil time (hrs)	Reference / Description
Np	Hematite <1 μm 0.2 g/L	Np(V) 1.9×10^{-7} M	Yucca Mt. well J-13 water	8.19	319	6	1	Runde *et al*. (2002) Np uptake was much less than Pu uptake by comparable minerals.
				8.19	435	8	24	
				8.19	682	12	50	
				8.19	556	10	90	
				8.19	747	13	240	
Np	Hematite 3g/L Aerobic	Np(V) 1×10^{-13} M	0.1 M $NaClO_4$	4	25	7	48	Jain *et al*. (2007) At pH < 5, the sorption of Np(V) onto hematite is negligible, beyond which the sorption sharply increases up to 90% at pH 10. Presence of humic acid decreases the sorption of Np(V) on hematite at higher pH, but this effect is negligible at lower pH. Under nitrogen and in presence of sodium dithionite, Np(V) is reduced to Np(IV) and sorption was enhanced at all pHs.
				6.2	94	22		
				7.5	1.16×10^3	77		
				9.6	3.83×10^3	92		
	Hematite 3g/L Humic acid 2 mg/L Aerobic	Np(V) 1×10^{-13} M	0.1 M $NaClO_4$	4	10	3	48	
				6.8	94	22		
				10.2	2.44×10^3	88		
	Hematite 3g/L Humic acid 2 mg/L Anaerobic	Np(IV) 1×10^{-13} M	0.1 M $NaClO_4$	4.1	222	40	48	
				5.6	1.18×10^3	78		
				7.9	1.63×10^4	98		
				9.5	6.33×10^3	95		
	Hematite 3g/L Anaerobic	Np(IV) 1×10^{-13} M	0.1 M $NaClO_4$	4.3	73	18	48	
				6.5	1.25×10^3	79		
				9.9	5.22×10^3	94		
Np	Amorphous Fe oxyhydroxide 0.89 g/L	Np(V) 4.5×10^{-11} M 4.7×10^{-12}	0.1 M $NaNO_3$	4	23	2	24	Girvin *et al*. (1991) At Np(V)
				5	183	14		
				6	2.89×10^3	72		

Radio-nuclide	Sorbents	Solution	Ion strength	pH	K_d (mL/g)	Sorp-tion (%)	Equil time (hrs)	Reference / Description
		M 4.5×10^{-13} M		7	2.7×10^{4}	96		concentration 4.5×10^{-13} M to 4.5×10^{-11} M, Np sorption onto amorphous Fe oxyhydroxide increases from pH 2 to pH 8. The aqueous NpO_2^+ species is dominant. To increase the Fe sorbent loading would shift the sorption edge toward lower pH.
				8	~1.11×10^{5}	~99		
				9	~1.11×10^{5}	~99		
	Amorphous Fe oxyhydroxide 0.89 g/L	Np(V) 4.7×10^{-12} M	0.1 M $NaNO_3$	4.2	~11	~1	24	
				5.1	336	23		
				6.0	3.37×10^{3}	75		
				7.0	2.14×10^{4}	95		
	Amorphous Fe oxyhydroxide 0.33 g/L	Np(V) 4.7×10^{-12} M	0.1 M $NaNO_3$	4.3	31	1	24	
				5.3	535	15		
				5.9	3.03×10^{3}	50		
				6.9	2.73×10^{4}	90		
				7.7	5.76×10^{4}	95		
	Amorphous Fe oxyhydroxide 0.09 g/L	Np(V) 4.7×10^{-12} M	0.1 M $NaNO_3$	4.1	227	2	24	
				5.2	709	6		
				5.8	2.78×10^{3}	20		
				6.9	2.59×10^{4}	70		
				7.8	1.0×10^{5}	90		
				9.0	1.1×10^{6}	99		

3.4 Americium

A summary of the americium sorption information (adsorption coefficient K_d, adsorption percentage, initial Pu concentration, pH, ion strength, equilibrium time, and sorbent loading) to iron oxyhydroxide phases is given in Table 4.

In an aqueous systems with 3×10^{-9} M Am(III) , Am sorption onto natural hematite is very strong and fast, a 100% Am sorption is achieved within 2 hours (Table 4). With Eu(III) 2×10^{-4} M in the aqueous systems, the sorption percentage or K_d of Am onto natural hematite increases with increasing pH from 2.5 to 5.7; at the same pH (5.7), the decrease in ion strength $NaNO_3$ from 0.1 M to 0.001 M or the increase in the content of fulvic acid from 0 to 20 mg/L will significantly increase the Am sorption onto natural hematite (Tao *et al*. 2006). Although fulvic acid will not be present in tanks, we include this information to demonstrate how strong complexing agents influence Am sorption to oxyhydroxides. At pH 5.5 or 8.0, Am(III) sorbes onto ferrihydrite surfaces as a bidentate corner-sharing species. Bidentate bonding indicates two bonds are formed between the solute and the surface. The implication of this to the PA is that the bond is strong and desorption is less likely to occur than in a monodentate system. Upon heating, ferrihydrite transforms to

goethite or hematite, the sorbed Am(III) at pH 5 is released from the sorbed samples during the transformation, but the sorbed Am(III) at pH 8 is partially incorporated into the ferrihydrite transformation products (Stumpf *et al*. 2006).

Table 4. Americium sorption to iron oxyhydroxide phases

Radio-nuclides	Sorbents	Solutions	Ion strength	pH	K_d (mL/g)	Sorp-tion (%)	Equil time (hrs)	Reference / Description
Am	Hematite V/m=400 ml/g	Am 1.1×10^{-9} M	0.1 M $CaCl_2$	4-6	~3.96×10^{4}	~99	~8	Tao *et al*. (2006) Without Eu, Am is completely up-taken by natural hematite rapidly. Am K_d onto hematite increases with (1) pH increase, (2) with fulvic acid (FA) increase at the same pH, and (3) with ion strength decrease at the same pH and FA concentration. Although FA may not be present in tanks, their interactions with Am is presented to demonstrate how a strong ligand interferes with hematite sorption.
	Hematite V/m=400 ml/g	Am 1.1×10^{-9} M Eu 2.1×10^{-4} M No FA	0.1 M $NaNO_3$	2.5	58			
	Hematite V/m=400 ml/g	Am 1.1×10^{-9} M Eu 2.1×10^{-4} M, No FA	0.1 M $NaNO_3$	5.7	246			
	Hematite V/m=400 ml/g	Am 1.1×10^{-9} M Eu 2.1×10^{-4} M FA 20 mg/L	0.1 M $NaNO_3$	5.7	2.38×10^{3}			
	Hematite V/m=400 ml/g	Am 1.1×10^{-9} M Eu 2.1×10^{-4} M No FA	0.01 M $NaNO_3$	5.7	3.6×10^{3}			
Am	Ferri-hydrite BET 235 m^2/g 1.5 g/L			~5.5	2.67×10^{3}	~80		Stumpf *et al*. (2006) Am sorbs as a bidentate corner-sharing species onto the surface

3.5 Technetium

A summary of the technetium sorption information (adsorption coefficient K_d, adsorption percentage, initial Pu concentration, pH, ion strength, equilibrium time, and sorbent loading) to iron oxyhydroxide phases is given in Table 5.

The sorption percentages of TcO_4^- species onto hematite, goethite, ferrihydrite and goethite-coated sand are very low and their K_d values are near zero in oxidizing conditions (Palmer *et al*. 1981, Kaplan 2003, Peretyazhko *et al*. 2009). However, in the aqueous reducing conditions, containing dissolved Fe(II), the Fe(III) oxyhydroxides such as hematite, goethite or ferrihydrite, can adsorb the Fe(II) and then promote the reduction of Tc(VII) to Tc(IV) (Peretyazhko *et al*. 2009). This latter phenomenon increases with increasing pH and is coincident with a second event of Fe(II) (aq) sorption (Peretyazhko *et al*. 2009). The reaction is almost instantaneous at pH 7. Tc(VII) reduction by Fe(II) is in the order: aqueous Fe(II) ~ adsorbed Fe(II) in phyllosilicate << structural Fe(II) in phyllosilicate << Fe(II) adsorbed on Fe(III) oxides – hematite and goethite (instantly). The reduced products are sorbed octahedral TcO_2 monomers and dimers with Fe(III) in the second coordination shell, indicating the Tc is incorporated into hematite or goethite structure (Peretyazhko *et al*. 2009).

Table 5. Technetium sorption to iron oxyhydroxide phases

Radio-nuclides	Sorbents	Solution	Ion strength	pH	K_d (mL/g)	Sorp-tion (%)	Equil time (hrs)	Reference / Description
Tc	Hematite BET 9 m^2/g 4.5 g/L	Tc 1.03×10^{-5} M	Fe(II) 1.0-1.2×10^{-4} M 0.03 M Na acetate	4.0	25	10	24	Peretyazhko *et al*. (2009) **Tc K_d onto hematite only is ~0.** Tc(VII) reduction by Fe(II): aqueous Fe(II) ~ adsorbed Fe(II) in phyllosilicate << structural Fe(II) in phyllosilicate << Fe(II) adsorbed on Fe(III) oxides – hematite and goethite (instantly). The reduced products are sorbed octahedral TcO_2 monomers and dimers with Fe(III) in 2th coordination shell – into hematite or goethite structure.
				4.0	36	14	96	
				4.0	36	14	192	
				4.5	161	42	24	
				4.5	544	71	96	
				4.5	~2.2×10^{4}	~99	192	
				5.0	2.25×10^{3}	91	24	
				5.0	~2.2×10^{4}	~99	96	
				5.6	~2.2×10^{4}	~99	24	
				5.8	~2.2×10^{4}	~99	24	
				6.1	~2.2×10^{4}	~99	24	
				6.5	~2.2×10^{4}	~99	24	
				7.0	~2.2×10^{4}	~99	24	
	Hematite BET 9 m^2/g 9 g/L	Tc 2.05×10^{-5} M	Fe(II) 2.3×10^{-4} M	7.0	~1.1×10^{4}	~99	24	
	Goethite BET 45 m^2/g 1.5 g/L	Tc 1.03×10^{-5} M	Fe(II) 1.2×10^{-4} M	7.0	~6.6×10^{4}	~99	24	
	Goethite 3.0 g/L	Tc 2.05×10^{-5} M	Fe(II) 2.3×10^{-4} M	7.0	~3.3×10^{4}	~99	24	
Tc	Sediment with Fe_2O_3 0.01%	TcO_4 stock	0.01 M $CaCl_2$	3.2	0.3		168	Kaplan (2003) K_d of TcO_4^- onto iron oxide-coated sediment is nearly zero.
				4.2	0.2			
				6.1	0.0			
				6.8	0.1			
	Sediment with Fe_2O_3 0.30%	TcO_4 stock	0.01 M $CaCl_2$	3.2	~0		168	
				4.2	~0			
				7.8	~0			
				8.8	~0			
Tc	Hematite	TcO_4 stock	0.1 M NaCl	4.1-9.1	5.4±1.2		504	Palmer and Meyer (1981)K_d of Tc onto hematite and magnetite are very low
	Magnetite	TcO_4 stock	0.1 M NaCl	4.3-9.3	0.8±0.8		504	

4.0 Conclusions

The objective of this report was to conduct a literature review to determine whether Pu, U, Np, Am and Tc would sorb to corrosion products on tank liners after the tank was filled with reducing grout (cementitious material containing slag to promote reducing conditions). There were no studies in the literature specifically designed to simulate SRS conditions of interest; *i.e.*, sorption to corrosion products of these radionuclides in the presence of reducing grout. One of the key ancillary parameters controlling sorption of these parameters is pH; this is especially true of Pu and U. A grouted tank pore water may have a pH >12 and is expected to maintain that pH for thousands of years. All literature sorption experiments were performed in pH <10.5 systems. Consequently some extrapolation is involved to predict what would happen in a cementitious – corrosion product environment of pH >12. Furthermore, few studies were found to investigate the radionuclides sorption under reducing conditions. In this document, information is tabulated about trends on how radionuclide sorbed with respect to ancillary parameters, such as pH, redox, radionuclide initial concentration, and solid phases. Based on the collected information, conclusions were then drawn to determine if conservative assumptions were made in existing PAs by not permitting Pu, U, Np, Am and Tc to sorb to corrosion products on tank liners.

It is likely that tank liner corrosion products would significantly sorb Pu. Based on the literature review, Pu tended to have increased sorption with increasing pH between pH 3 and 10. At pH 10, Pu consists of carbonate and/or hydroxide complexes. It appears that the iron oxyhydroxide solid phases out compete these complexes in the aqueous phase for the Pu to promote Pu sorption; however, the carbonate alkalinity of >100 meq/L would decrease the Pu sorption onto goethite (α-FeOOH) (Sanchez *et al*. 1985).

It is unlikely that tank liner corrosion products would retain much uranyl, UO_2^{2+}, U in the oxidized state. Unlike Pu-hydroxy/carbonate complexes, it appears that uranyl forms complexes at higher pH values that are resistant to sorption by Fe-oxyhydroxides. Several studies conducted at pH 8 to 10 demonstrated that uranyl sorption decreased compared to lower pH systems. However, tank grout will create reducing conditions that will promote the reduction of UO_2^{2+} to U(IV) and by virtue of its tetra-valence, much greater total U sorption to corrosion products would be expected under reducing conditions. Information is lacking on how U(IV) would sorb to corrosion products at high pH; this is a specific area where experimental data may be especially useful.

Due to its higher stable oxidation state Np as neptunyl, (Np(V), NpO_2^+) not surprisingly sorbs appreciably less than Pu(IV) to iron oxyhydroxides. As the pH increased between 5 and 10 the K_d values of neptunyl increased significantly. Additionally, there was no experimental data to indicate that the Np K_d values declined at higher pH values as was observed with uranyl due to carbonate complexes; however, some modeling work indicated the decreased adsorption of Np at higher pH (Wang and Anderko, 2001). Tank grout may promote reducing conditions, which may promote reduction of Np(V) to Np(IV) and therefore greater sorption to corrosion products. Information is lacking on how Np(IV) would sorb to corrosion products at high pH values.

Americium sorbs strongly at high pH values. There was an exceptionally strong pH dependence, as sorption K_d values increased from double digits to four or five digits as the pH increased from 3 to >8. Americium is not a redox sensitive element and therefore the K_d values would be approximately the same under reducing and older grout that has become oxidized.

Pertechnetate, TcO_4^-, would not be retained by corrosion products due to surface charge repulsion of the Fe-oxyhydroxide at high pH and high competing anion concentrations. However, under reducing conditions, the TcO_4^- would readily convert to Tc(IV) and again, the tetravalent cation, Tc(IV), would be expected to sorb strongly under reducing conditions to the Fe-oxyhydroxides at high pH values. We are not aware of any Tc(IV) sorption experiments conducted at elevated pH values with Fe oxyhydroxides.

The literature review provided insight into the sorption behavior of the radionuclides under oxidizing conditions. Namely, under oxidizing tank conditions, Tc and U sorption to corrosion products is unlikely, whereas significant amount of Pu, Am, and to a lesser extent Np sorption will likely occur. There was little information about sorption (except Pu(IV)) behavior of these radionuclides under reducing conditions. Reducing conditions are expected to exist initially at the bottom of the tanks because about 8 m of reducing grout will be placed in the tank residual radionuclides (tank heel). This is of particular interest because Tc, Np, and U are likely to reduce to stronger sorbing forms, tetravalent forms. It is very possible that these tetravalent radionuclides would adsorb to corrosion products or simply precipitate in solution. Based on first principles of geochemistry (Sposito, 1984) and expected speciation of high pH geochemistry of cement leachate (Wang *et al.* 2009) it is expected that tetravalent metals would indeed sorb to these corrosion products; however testing under site specific conditions are necessary to confirm this expectation.

The present PA does not include any sorption to corrosion products in its conceptual geochemical model. Based on this literature review, it is a conservative assumption in the present PA not to include Pu, Am, and Np sorption to corrosion products. It is a conservative assumption in the present PA not to include Tc and U sorption during the period that the tanks are reduced (the first two aging stages); however laboratory information is necessary to confirm this expectation. It is reasonable for the PA to omit Tc and U sorption during oxidizing conditions (older grout).

5.0 References

Aamrani, S.E., Giménez, J., Rovira, M., Seco, F., Grive, M., Bruno, J., Duro, L., and De Pablo, J., A spectroscopic study of uranium (VI) interaction with magnetite. *Applied Surface Sci*. **2007**, *253*, 8794-8797.

Bargar, J.R., Reitmeyer, R., Lenhart, J.J., and Davis, J.A., Characterization of U(VI)-carbonate ternary complexes on hematite: EXAFS and electrophoretic mobility measurements. *Geochim Cosmochim. Acta* **2000**, *64*, 2737-2749.

Carbol, P. and Engkvist, I., Compilation of radionuclide sorption coeffi cients for performance assessment. *SKB rapport R-97-13*, Swedish Nuclear Fuel and Waste Management Co, **1997**.

Duff, M.C., and Amrhein, C., Uranium(VI) sorption on goethite and soil in carbonate solutions. *Soil Sci. Soc. Am. J*. **1996**, *60*, 1393-1400.

Duff, M.C., Coughlin, J.U., and Hunter, D.B., Uranium co-precipitation with iron oxide minerals. *Geochim Cosmochim. Acta* **2002**, *66*, 3533-3547.

Duro, L., Aamrani, S.E., Rovira, M., De Pablo, J., and Bruno, J., Study of the interaction between U(VI) and the anoxic corrosion products of carbon steel. *Applied Geochem*. **2008**, *23*, 1094-1100.

Ferris, F.G., Hallberg, R.O., Lyvén, B., and Pedersen, K., Retention of strontium, cesium, lead and uranium by bacteria iron oxides from a subterranean environment. *Applied Geochem*. **2000**, *15*, 1035-1042.

Girvin, D.C., Ames, L.L., Schwab, A.P., and McGarrah, J.E., Neptunium sorption on synthetic amorphous iron oxyhydroxide. *J. Colloid and Interface Sci*. **1991**, *141*, 67-78.

Hiemstra, T., Van Riemsdijk, W.H., Rossberg, A., and Ulrich, K.U., A surface structural model for ferrihydrite II: Adsorption of uranyl and carbonate. *Geochim Cosmochim. Acta* **2009**, *73*, 4437-4451.

Hixon, A. E. Hu, Y. Kaplan, D.I., Kukkadapu, R. K., Nitsche, H., Qafoku, O., and Powell, B. A., Influence of iron redox transformations on plutonium sorption to sediments. *Radiochimica Acta* **2010**, *98*, 685-692.

Hsi, C.K.D., and Langmuir, D., Adsorption of uranyl onto ferric oxyhydroxides: Application of the surface complexation site-binding model. *Geochim Cosmochim. Acta* **1985**, *49*, 1931-1941.

Jain, A., Rawal, N., Kumar, S., Tomar, B.S., Manchanda, V.K., and Ramanathan, S., Effect of humic acid on sorption of neptunium on hematite colloids. *Radiochimica Acta* **2007**, *95*, 501-506.

Kaplan D.I., Powell, B.A., Gumapas, L., Coates, J.T., Fjeld, R.A., and Diprete, D.P., Influence of pH on plutonium desorption/solubilization from sediment. *Environ. Sci. Technol*. **2006**, *40*, 5937-5942.

Kaplan, D.I., Influence of surface charge of a Fe-oxide and an organic matter dominated soil on iodide and pertechnetate sorption. *Radiochim. Acta* **2003**, *91*, 173-178.

Kersting, A.B., Zhao, P.H., Zavarin, M., Sylwester, E.R., Allen, P.G., and Williams, R.W., Sorption of Pu(V) on Mineral Colloids. In *Colloid-facilitated transport of low-solubility radionuclides: A field, experimental, and modeling investigation*. (Ed. Kersting, A.B., and Reimus, P.W.), *UCRL-ID-149688*, Lawrence Livermore National Laboratory, **2003**, 67-87.

Liger, E., Charlet, L., and Van Cappellen, P., Surface catalysis of uranium(VI) reduction by iron(II). *Geochim Cosmochim. Acta* **1999**, *63*, 2939-2955.

Lu, N., Triay, I.R., Cotter, C.R., Kitten, H.D., and Bentley, J., Reversibility of Sorption of Plutonium-239 onto Colloids of Hematite, Goethite, Smectite, and Silica. *LA-UR-98-3057*, Los Alamos National Laboratory, **1998**.

Lu, N., Reimus, P.W., Parker, G.R., Conca, J.L., and Triay, I.R., Sorption kinetics and impact of temperature, ionic strength and colloid concentration on the adsorption of plutonium-239 by inorganic colloids. *Radiochimica Acta* **2003**, *91*, 713-720.

Mahoney, J.J., Cadle, S.A., and R.T., Jakubowski, Uranyl sorption onto hydrous ferric oxide-A re-evaluation for the diffuse layer model database. *Environ. Sci. Technol*. **2008**, *43*, 9260-9266.

Missana, T., García-Gutiérrez, M., and Maffiotte, C., Experimental and modeling study of the uranium(VI) sorption on goethite. *J. Colloid Interface Sci*. **2003**, *260*, 291-301.

Moyes, L.N., Parkman, R.H., Charnock, J.M., Vaughan, D.J., Livens, F.R., Hughes, C.R., and Braithwaite, A., Uranium uptake from aqueous solution by interaction with goethite, lepidocrocite, muscovite and mackinawite: Am X-ray absorption spectroscopy study. *Environ. Sci. Technol.* **2000**, *34*, 1062-1068.

Nico, P.S., Steward, B.D., and Fendorf, S., Incorporation of oxidized uranium into Fe (Hydr)oxides during Fe(II) catalyzed remineralization. *Environ. Sci. Technol*. **2009**, *43*, 7391-7396.

Palmer, D.A., and Meyer, R.E., Sorption of technetium on selected inorganic ion-exchange materials and on a range of naturally occurring minerals under oxic conditions. *J. Inorg. Nucl. Chem.* **1981**, *43*, 2979-2984.

Payne, T.E., Brendler, V., Comarmond, M.J., and Nebelung, C., Assessment of surface area normalization for interpreting distribution coefficient (K_d) for uranium sorption. *J. Environ. Radioactivity* **2011**, *102*, 888-895.

Payne, T.E., Uranium(VI) interaction with mineral surfaces: Controlling factors and surface complexation modeling, *Ph.D. Dissertation*, University of New South Wales, **1999**.

Payne, T.E., Lumpkin, G.R., and Waite, T.D., Uranium^{VI} sorption on model minerals. In *Sorption of Metals by Geomedia* (Ed. E.A. Jenne), **1998**, 75-97.

Peretyazhko, T., Zachara, J.M., Heald, S.M., Jeon, B.H., Kukkadapu, R.K., Liu, C., Moore, D., and Resch, C.T., Heterogeneous reduction if Tc(VII) by Fe(II) at the solid-water interface. *Geochim. Cosmochim. Acta* **2009**, *72*, 1521-1539.

Powell, B. A., Fjeld, R. A., Kaplan, D. I., Coates, J. T., and Serkiz, S. M., $Pu(V)O^{2+}$ sorption and reduction by synthetic hematite and goethite. *Environ. Sci. Technol*. **2005**, *39*, 2107-2114.

Powell, B. A., Fjeld, R. A., Kaplan, D. I., Coates, J. T., and Serkiz, S. M., $Pu(V)O^{2+}$ Sorption and reduction by synthetic magnetite (Fe_3O_4). *Environ. Sci. Technol*. **2004**, *38*, 6016-6024.

Reich, T., Moll, H., Arnold, T., Denecke, M.A., Herring C., Geipel, G., Bernard G., Nitsche, H., Allen, P.G., Bucher, J.J., Edelstein, N.M., and Shuh, D.K., An EXAFS study of uranium (VI) sorption onto silica gel and ferrihydrite. *J. Electron Spect. Rel. Phenom*. **1998**, *96*, 237-243.

Romanchuk, A. Y., Kalmykov, S. N., and Aliev, R. A., Plutonium sorption onto hematite colloids at femto-and nanomolar concentrations. *Radiochimica Acta* **2011**, *99*, 137-144.

Rossberg A., Ulrich, K.U., Weiss, S., Tsushima, S., Hiemstra, T., and Scheinost, A.C., Identification of uranyl surface complexes on ferrihydrite: Advanced EXAFS data analysis and CD-MUSIC modeling. *Environ. Sci. Technol*. **2009**, *43*, 1400-1406.

Rovira, M., Aamrani, S.E., Duro, L., Giménez, J., De Pablo, J., and Bruno, J., Interaction of uranium with in situ anoxically generated magnetite on steel. *J. Hazard. Mat*. **2007**, *147*, 726-731.

Runde, W., Conradson, S. D., Efurd, D. W., Lu, N., VanPelt, C. E., and Tait, C. D., Solubility and sorption of redox-sensitive radionuclides (Np, Pu) in J-13 water from the Yucca Mountain Site: Comparison between experiment and theory. *Appl. Geochem*. **2002**, *17*, 837-853.

Sanchez, A. L., Murray, J. W., and Sibley, T. H., The sorption of plutonium IV and V on goethite. *Geochim. Cosmochim. Acta* **1985**, *49*, 2297.

Sherman, D.M., Peacock, C.L., and Hubbard, C.G., Surface complexation of U(VI) on goethite (α-FeOOH). *Geochim. Cosmochim. Acta* **2008**, *72*, 298-310.

Sposito, G., *The surface chemistry of soils.* New York, NY, Oxford University Press, **1984**.

Stewart, B.D., Mayes, M.A., and Fendorf, S., Impact of uranyl-calcium-carbonate complexes on uranium(VI) sorption to synthetic and natural sediment. *Environ. Sci. Technol*. **2010**, *44*, 928-934.

Stewart, B.D., Amos, R.T., Nico, P.S. and Fendorf, S., Influence of uranyl speciation and iron oxides on uranium biogeochemical redox reaction. *Geomicrobiol. J.* **2011**, *28*, 444-456.

Stumpf, S., Dardenne, K., Hennig, C., Foerstendorf, H., Klenze, R., and Fanghänel, T., Sorption of Am(III) onto 6-line-ferrihydrite and its alteration products: Investigation by EXAFS. *Environ. Sci. Technol.* **2006**, *40*, 3522-3528.

Tao, Z.Y., Chu, T.W., Li, W.J., Du, J.Z., Dai, X.X., and Gu, Y.J., Cation sorption of NpO_2^+, UO_2^{2+}, Zn^{2+}, Sr^{2+}, Yb^{3+}, and Am^{3+} onto oxides of Al, Si, and Fe from aqueous solution: ionic strength effect. *Colloids and Surface Sci. A: Physicochem. Eng. Aspects* **2004**, *242*, 39-45.

Tao, Z.Y., Li, W.J., Zhang, F.M., and Han, J., Sorption of Am(III) on red earth and natural hematite. *J. Radioanal. Nucl. Chem*. **2006**, *268*, 563-568.

Waite, T.D., Davis, J.A., Payne, T.E., Waychunas, G.A., and Xu, N., Uranium(VI) sorption to ferrihydrite: Application of a surface complexation model. *Geochim. Cosmochim. Acta* **1994**, *58*, 5465-5478.

Wang, P.M., and Anderko, A. Thermodynamic modeling of the adsorption of radionuclides on selected minerals. I: Cations. *Ind. Eng. Chem. Res*. **2001**, *40*, 4428-4443.

Wang, L., E. Martens, D. Jacques, P. Decanniere, J. Berry, D. Mallants. Review of sorption values for the cementitious near field of a near surface radioactive waste disposal facility. Mol, Brussels, ONDRAF/NIRAS, **2009**.

Wiersma, B.J., and Subramanian, K.H., Corrosion testing of Carbon Steel in Acid Cleaning Solutions. WSRC-TR-2002-00427, Washington Savannah River Company, Aiken, SC, **2002**.

Zeng, H., Singh, A., Basak, S., Ulrich, K.U., Sahu, M., Biswas, P., Catalano, J.G., and Giammar, D.E., Nanoscale size effects on uranium(VI) sorption to hematite. *Environ. Sci. Technol*. **2009**, *43*, 1373-1378.

Distribution:

P. M. Almond, 773-43A – Rm. 227
A. B. Barnes, 999-W – Rm.336
H. H. Burns, 773-41A – Rm.214
B. T. Butcher, 773-43A – Rm.212
L. B. Collard, 773-43A – Rm.207
D. A. Crowley, 773-43A – Rm.216
S. D. Fink, 773-A – Rm.112
G. P. Flach, 773-42A – Rm.211
B. J. Giddings, 786-5A – Rm.2
J. C. Griffin, 773-A – Rm. A-202
C. C. Herman, 999-W – Rm. 344
R. A. Hiergesell, 773-43A – Rm.218
G. K. Humphries, 705-3C – Rm.206
P. R. Jackson, 703-46A – Rm. 223
D. I. Kaplan, 773-43A – Rm.215
D. Li, 999-W – Rm.336
S. L. Marra, 773-A – Rm. A-230
J. J. Mayer, 773-42A – Rm. 242
A. M. Murray, 773-A, Rm. A-229
F. M. Pennebaker, 773-42A – Rm.146
S. H. Reboul, 773-A, Rm. B-132
K. A. Roberts, 773-43A – Rm.225
K. H. Rosenberger, 705-1C – Rm.33b
F. G. Smith, III 773-42A – Rm.178
K. H. Subramanian, 766-H – Rm.2204

(1 file copy & 1 electronic copy), 773-43A – Rm.213